Energy Conversion and Management 342 (2025) 120070

Contents lists available at ScienceDirect

Energy Conversion and Management

journal homepage: www.elsevier.com/locate/enconman

Potential of thermal energy storage for endothermic reconversion of hydrogen carriers

Thomas Bauer [a,*], Marco Prenzel [a], Shigehiko Funayama [b], Yukitaka Kato [b]

[a] German Aerospace Center (DLR), Institute of Engineering Thermodynamics, Linder Hoehe, 51147 Cologne, Germany
[b] Institute of Science Tokyo, Institute of Integrated Research, Laboratory for Zero-Carbon Energy, 2-12-1-N1-22, Ookayama, Meguro-ku, Tokyo 152-8550, Japan

ARTICLE INFO

Keywords:
Ammonia
Dibenzyl toluene
Methane
Liquefied natural gas
Methanol
Molten salt

ABSTRACT

In resource-poor industrial countries with high energy consumption, a significant proportion of future energy will likely be imported by ships using chemical hydrogen carriers. The considered hydrogen (H_2) derivatives – liquefied natural gas, methanol, liquid organic hydrogen carriers, and ammonia – undergo considerable conversion losses during endothermic reconversion to H_2 in the importing country. Currently, these losses have been accepted and scientific research on approaches to increase conversion efficiency remains limited. This study introduces a novel concept for externally supplying conversion heat using local renewable electricity through a power-to-heat and high-temperature thermal energy storage system (HT-TES-P2H system). The advantages and disadvantages, along with key figures for the four H_2 derivatives, as well as the thermal and process-related integration of an HT-TES-P2H system into the endothermic processes, were analysed systematically. Suitable heat integration concepts were identified for all four H_2 carriers; ammonia was thermodynamically modelled in detail. For ammonia a majority of the endothermic heat can be provided by an HT-TES-P2H system and hydrogen yield increases from 80 to 96 %. Japanese and German energy systems were analysed to identify potential savings and suitable locations for implementing the concept. A simplified capital cost analysis was carried out for ammonia production in Brazil and Australia with import to Germany. Overall, our novel concept indicates that the addition of a relatively inexpensive HT-TES-P2H system in the importing country results in significantly greater capital expenditure savings of 16.7 % by reducing the size of the entire ammonia supply chain.

1. Introduction

The implementation of a hydrogen (H_2) economy is perceived as a prerequisite for achieving climate targets. Currently, approximately 96 % of global hydrogen production relies on fossil fuels, contributing to substantial greenhouse gas (GHG) emissions [1]. In the energy sector, the production of H_2 and H_2-based fuels is expected to increase from <90 million tonnes in 2020 to 530 million tonnes in 2050 in a net zero scenario [2]. A future sustainable H_2 supply therefore requires both a switch from fossil to renewable H_2 production and a sharp increase in production volumes. Several sustainable methods of H_2 production are known. They include biomass processes, such as biogas reforming, pyrolysis, gasification, and fermentation, as well as water splitting processes, such as electrolysis, thermolysis, and photolysis utilising solar and wind energy, combined with hydropower and geothermal energy [1,3,4].

Among the sustainable H_2 generation methods, water electrolysis with renewable electricity is the most widespread and has the highest conversion efficiency [1]. Electrolysis requires considerable electricity quantities and, ideally, a constant supply of electricity. In the future, a large proportion of this electricity will be produced by wind and photovoltaic (PV) systems. Regions in Europe, South Korea, Japan (JP), and parts of China will likely have insufficient resources to produce the necessary H_2 themselves, and are therefore considered H_2 demand centres [5,6]. These countries face limitations, such as the potential for wind and solar energy (including full load hours per year, and seasonality) and available land area. The demand for H_2 arises in sectors such as power generation, the process industry, basic materials, petrochemicals, shipping, aviation and heavy goods transport [7]. To achieve a climate-neutral supply, these countries plan to import considerable quantities of H_2. Countries with high wind and PV potential are preferred as export sources because they have the capability to produce low-cost H_2.

H_2 transport and storage are challenging due to the low volumetric energy density of H_2. Hence, H_2 must be compressed, liquefied, or

* Corresponding author.
E-mail address: thomas.bauer@dlr.de (T. Bauer).

https://doi.org/10.1016/j.enconman.2025.120070
Received 11 January 2025; Received in revised form 29 May 2025; Accepted 10 June 2025
Available online 8 July 2025

Nomenclature

Acronyms

AT	Autothermal
CAPEX	Capital expenditure
CCS	Carbon capture and storage
CCU	Carbon capture and utilisation
CH_2	Compressed hydrogen
CLP	Classification, labelling, and packaging
DAC	Direct air capture
DBT	Dibenzyl toluene
DE	Germany
EU	European Union
Ebsilon	EBSILON®Professional software
e-LNG	Liquefied synthetic methane
GHG	Greenhouse gas
GHS	Globally harmonised system of classification and labelling of chemicals
HTF	Heat transfer fluid
HT	High-temperature
HX	Heat exchanger
IEA	International Energy Agency
JP	Japan
LH_2	Liquefied hydrogen
LHV	Lower heating value
LNG	Liquefied natural gas
LOHC	Liquid organic hydrogen carriers
LT	Low-temperature
MeOH	Methanol
NO_x	Nitrogen oxide gases
P2H	Power-to-heat
PCM	Phase change material
PEM	Proton exchange membrane
POX	Partial oxidation
PSA	Pressure swing adsorption
PV	Photovoltaics
R&D	Research and technology development
SoA	State-of-the-art
SR	Steam reforming
TCS	Thermochemical storage
TES	Thermal energy storage
TRL	Technology readiness level
WGS	Water gas shift

Symbols

F_{H2}	Molar flow of hydrogen
$F_{Carrier}$	Molar flow of H_2 carrier
h	Specific energy consumption per hydrogen mass
$h_{NH3,heat}$	Specific ammonia heat consumption
h_{Pel}	Specific electricity consumption
$h_{\dot{Q},TES}$	Specific heat supply of the TES-P2H system
$h_{\dot{Q},amb}$	Specific ambient heat supply
$H_{H_2,LHV}$	Lower heating value of hydrogen
$H_{NH_3,LHV}$	Lower heating value of ammonia
$\dot{m}_{H_2}^{product}$	Mass flow of hydrogen product
$\dot{m}_{NH_3}^{feed}$	Mass flow of ammonia feed for conversion and heat supply
$\dot{m}_{NH_3\rightarrow H_2}^{feed}$	Mass flow of ammonia feed for conversion
$\dot{m}_{NH_3,heat}^{feed}$	Mass flow of ammonia feed for heat supply
M_{H2}	Molar mass of hydrogen
M_{NH3}	Molar mass of ammonia
P_{el}	Electrical power consumption
$\dot{Q}_{TES}$	Heat flow from TES-P2H system
$\dot{Q}_{amb}$	Ambient heat flow
X	Stoichiometric coefficient
$\eta_{E,NH3}$	Energy efficiency of NH_3 to H_2 conversion based on the LHV
$\eta_{E,total}$	Energy efficiency of NH_3 to H_2 conversion based on the LHV with electrical power and heat flow from the TES-P2H system
$\eta_{E,total*}$	$\eta_{E,total}$ for 6000 h the 'progressive' and 2000 h 'best guess' cases
$\eta_{el\rightarrow H2}$	Efficiency of water electrolysis
$\eta_{H2\rightarrow NH3}$	Efficiency of ammonia synthesis
η_{H2}	Hydrogen yield
$\eta_{H2,NH3}$	Hydrogen yield of ammonia reconversion/cracking
$\eta_{NH3,Transp}$	Ammonia transport efficiency

converted into other molecules for economical storage or transportation. Various options are available for the transport of H_2. Transport by truck, rail, and inland waterways is typically attractive only for small quantities and short distances using compressed hydrogen (CH_2), liquefied hydrogen (LH_2), or H_2 derivatives. Other H_2 storage options, such as metal hydrides, physisorption, and cryo-compressed H_2, also exist. These options are not considered in detail herein due to their high cost, increased transportation weight, and other properties, which make them unsuitable for long-distance transport [8]. Liquid synthetic fuels (e-fuels) can also be produced using renewable electricity, water, and CO_2 (e.g., the Fischer-Tropsch process). E-fuels can also be transported and used directly without reconversion in industries such as transportation, industrial processes, and power generation. Hence, in this study, e-fuels, for which reconversion to H_2 appears unattractive, were excluded [3,9,10].

Various studies have assumed that importing H_2 over medium distances, on the order of 5000 km, via pipelines with CH_2 is the most favourable option (especially if existing natural gas pipelines can be converted for this purpose). The disadvantages of these pipelines include considerable infrastructure costs, long construction times, and long-term commitments. Deep-sea ship transport is preferred over pipelines over longer distances via sea routes [5,7,11,12].

LH_2 is considered a major mode of transportation for deep-sea ship transport. The advantages include a high gravimetric energy density, high H_2 utilisation rate, stable gas purity, and the potential utilisation of cold during regasification. LH_2 also faces several challenges. One of the primary disadvantages is the extremely low storage temperature (−253 °C at atmospheric pressure). This requires energy-intensive liquefaction and specialised (expensive) infrastructure for these low temperatures. This also leads to significant boil-off losses on ships (reported values range from 0.05 to 1 %/day), as well as during both loading and unloading at the port, which must be compensated. Molecular H_2 exists in two isomeric forms: *ortho*-H_2 and *para*-H_2. This conversion requires additional energy and must be safely controlled when using LH_2. Further details on these forms are provided in a review article [13]. Moreover, H_2 is highly flammable and requires stringent safety measures to prevent leakage and explosion. Although LH_2 has a high gravimetric energy density, it has a comparatively low volumetric energy density (71 kg-H_2/m^3) compared to that of H_2 derivatives. Certain pilot projects do exist (e.g., the Kawasaki demonstration in JP [14]); however LH_2 technology for charging, shipping, and discharging has not been implemented on a large scale, with no current global trading market for LH_2.

This study selected H_2 derivatives as attractive options for the transport of H_2 by ships in the deep sea. Compared to LH_2, H_2 derivatives offer the possibility of chemically binding molecular H_2, making it easier

to transport and store over longer distances and durations. For example, moderate temperatures and pressures can be used, and technologies available for transport and storage can be employed. The major H_2 derivative options are ammonia (NH_3), methanol (MeOH), liquid organic hydrogen carriers (LOHC), and liquified natural gas (LNG). LNG can be replaced by liquefied synthetic methane (e-LNG) in the future [6,15,16]. There are various definitions of LOHC in the literature. In this study, liquid media, such as the selected oil example, dibenzyl toluene (DBT), which are transported back and forth by ship between ports with repeated H_2 charge/discharge cycles, are referred to as LOHC. Subsection 4.2 provides a more detailed overview of the selected H_2 derivatives (see also Table 3).

High conversion losses occur along the H_2 supply chain with H_2 electrolysis and the synthesis and reconversion of H_2 derivatives [17,18]. A common feature and major disadvantage of the selected H_2 derivatives (NH_3, MeOH, LOHC, and LNG) is that their reconversion from the H_2 derivatives to H_2 is an endothermic process in the importing country. Depending on the H_2 derivative, the theoretical reaction heat, along with the feed (and water) evaporation heat, ranges from 18 to 27 % of the lower heating value (LHV) of the produced H_2 (Table 3). This heat is typically provided by the combustion of the H_2 derivatives, process off-gases, or the produced H_2. There is generally only limited scientific work on the integration of external heat sources to increase the efficiency of the reconversion of H_2 derivatives. Possible external sources include concentrating solar, environmental, and waste heat (e.g., from process industry and fuel cell) [16,19,20]. Environmental heat can be used to vaporise the liquid H_2-carriers. If the H_2 derivatives are converted to generate electricity in power cycle processes, there are also opportunities to increase efficiency through process integration [19] and the incorporation of waste and solar heat [21,22]. The integration of an alternative external heat source for the reconversion of chemical energy carriers to H_2 will likely lead to a lower amount of H_2 derivate import and hence allow downsizing with capital cost savings along the entire H_2 chain. That is, the installed size of wind and/or PV power, electrolysers, synthesis and shipping should be reduced by utilising external heat sources (Fig. 1).

Research has strongly focused on the development of reconversion processes (e.g., catalyst development and reactor design). The benefits of heat integration for increasing the efficiency of the process chain for H_2 production are less apparent in current research. Only a few studies have considered the integration of thermal energy storage (TES) systems for the endothermic reconversion of chemical energy carriers [9,23]. As the external heat sources under consideration (e.g., solar heat and waste heat) are not constantly available, the use of TES is of fundamental importance. Previous publications have focused on the transfer of thermal energy between the LOHC-charge and -discharge process via TES [9] and the temporal stabilisation of industrial waste heat with TES for LOHC discharge [23].

The novel concept proposed in this study – sector coupling with volatile renewable electricity, power-to-heat (P2H) and high-temperature (HT) TES technologies, collectively defined as the HT-TES-P2H concept – is only currently known in other fields, such as the chemical industry [24,25] (Fig. 1). The theoretical, technical, and economic potential of ambient low-temperature (LT) and HT external heat integration for endothermic reconversion processes of different chemical energy carriers (e.g., LOHC, NH_3, MeOH, and LNG) in importing countries, such as JP and Germany (DE), has not yet been assessed and is the subject of this study. In addition to the integration of ambient heat, this study focuses on sector coupling with local volatile renewable electricity, which is continuously supplied to the process as heat via the HT-TES-P2H system. Among the four H_2 derivatives considered, the focus is on NH_3.

The aim of this study was to minimise the internal heat supply via combustion, instead supplying heat externally, to achieve a high H_2 yield and reduce the quantity of H_2 carrier imports.

2. Overall methodology

The remainder of this paper is organised into three sections. For the proposed HT-TES-P2H concept, Section 3 summarises relevant energy information related to the current status, future policies, renewable energy implementation, and H_2 import of JP and DE. The differences and similarities between the JP and DE energy systems are analysed, and the theoretical potential of the proposed HT-TES-P2H concept, shown in Fig. 1, is determined.

Section 4 provides an assessment of the four H_2 carriers, the H_2 reconversion process and the related subcomponents (P2H and TES). Subsection 4.1 first provides background information on HT-P2H and HT-TES technologies, such as their temperature operating range and market status. Subsection 4.2 provides a comparative overview of the four H_2 carriers – LOHC, NH_3, MeOH and LNG – highlighting their advantages, disadvantages, and key figures. Subsection 4.3 presents an analysis of the endothermic reconversion process for each H_2 carrier and develops an overall heat integration concept with P2H and TES. NH_3 crackers are then selected and analysed in more detail.

In Section 5, the proposed HT-TES-P2H concept (Fig. 1) for NH_3 is thermodynamically implemented in the EBSILON®Professional Release 15.02 (Ebsilon) software and analysed in different configurations [26]. Initially, efficiencies and different specific consumptions are defined. First, in Subsection 5.1, a literature model is validated using Ebsilon. Subsection 5.2 defines a reference 'best guess' case based on large-scale industrial NH_3 cracker developments. The analysed cases, with external heat integration, are described in Subsection 5.3 and compared with the 'best guess' case in terms of their technical potential. In addition to the proposed HT-TES-P2H concept with NH_3, the integration of ambient heat is analysed. Subsection 5.4 estimates the economic potential of the

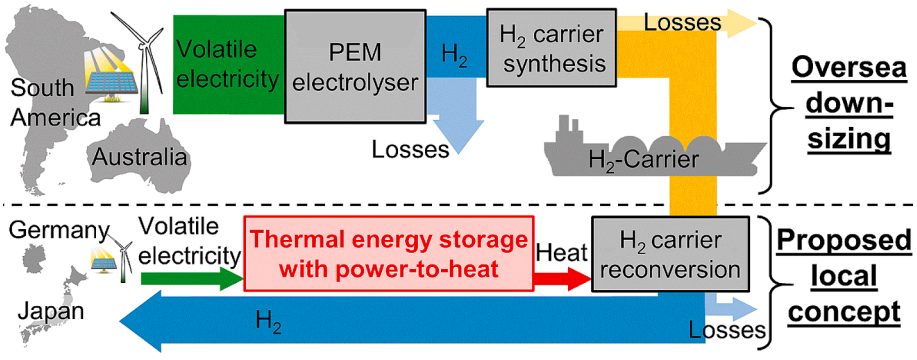

Fig. 1. Schematic of the proposed and analysed HT-TES-P2H concept for heat integration to reduce the H_2 supply chain in size with the selected countries of Japan and Germany. PEM, proton exchange membrane.

HT-TES-P2H concept for NH_3.

Section 6 summarises the results and draws conclusions regarding the theoretical, technical, and economic potential of the proposed HT-TES-P2H concept with NH_3 for JP and DE.

As Sections 3, 4, and 5 cover different topics, the detailed methodology was described at the beginning of each section to ensure a logical flow of reading.

3. Results and discussion of country assessment and theoretical potential

3.1. Japan

Fig. 2 shows the **current** total energy flow in terms of supply and consumption in JP for 2022 [27]. The current strong focus on fossil fuels is clearly visible. The transition from fossil fuel resources to renewable energy has progressed, particularly in terms of electricity generation. In JP, all commercial nuclear power plants were shut down after the Great East JP Earthquake in 2011 for safety inspections and upgrades [28]. Since then, nuclear reactors have been gradually restarted. The (primarily grey) H_2 supply was approximately 240 PJ/year (2 million tonnes/year) in 2021 [29]. The NH_3 demand is currently approximately 20 PJ/year (1 million tonnes/year) [30]. The MeOH market is currently approximately 40 PJ/year (approximately 2 million tonnes/year). JP imports a significant proportion of its energy as LNG with a value of 3350 PJ/year (67 million tonnes/year) in 2023 [27,31].

The Japanese government has set **interim** energy policy targets as outlined in the 6th Strategic Energy Plan, announced in 2021 [29]. GHG emissions are planned to be reduced by 46 % by 2030 compared with 2013 levels. The goal is to further increase the share of electricity generation by 2030 as follows: nuclear energy to 20–22 %, renewable energy to 36–38 % and NH_3/H_2-based power generation to 1 %. Another aim is to increase the (mostly grey) H_2 supply to 360 PJ/year (3 million tonnes/year) by 2030. The domestic demand for NH_3 as fuel is estimated to be approximately 56 PJ/year (3 million tonnes/year) by 2030. Another aim is to inject 1 % synthetic methane into the existing natural gas infrastructure. Shipbuilding and the shipping of LNG, LH_2, and NH_3 are set to be strengthened. A commercial demonstration of a zero-carbon ship is planned for 2028 [29,32]. Additionally, a draft of the 7th Strategic Energy Plan was published in December 2024 [33]. Compared with the 6th Strategic Energy Plan, the 7th Strategic Energy Plan mentions the introduction of TES as a demand-response measure to improve the flexibility of the electricity system. Demand-response in the electricity grid can be achieved by coupling the TES via a P2H system, whereby the P2H system is operated flexibly for the electricity grid.

The Japanese government aims to achieve carbon neutrality by **2050**. The domestic demand for NH_3 as fuel is presumed to be approximately 560 PJ/year (30 million tonnes/year) by 2050. The goal is to replace 90 % of natural gas with synthetic methane by 2050. It is expected that the H_2 supply will increase to 2400 PJ/year (20 million tonnes/year) by 2050 [29]. JP's Green Growth Strategy Towards Carbon Neutrality 2050′ estimated an increase in electricity demand of 30–50 % and established a scenario of 50–60 % renewables in the electricity mix by 2050 [34].

Due to its geography, JP faces distinct challenges with respect to the expansion of **renewables**, with mountainous terrain limiting its potential for onshore renewables. JP already has the highest installed solar energy capacity per square metre of flat land worldwide. Additionally, due to the steeply sloping coastline, non-floating offshore wind turbines are almost exclusively feasible in low-lying marine areas. JP is increasingly focusing on floating offshore wind energy. Bogdanov et al. [35] concluded that the renewable capacity could be relatively evenly distributed across JP. Solar PV dominates the western, central, and southern regions, and is located closer to major cities. The northern and western regions, which have relatively low population densities, have high onshore wind potential with limited consumers in the area. It is projected that the electricity grid will transmit wind power generated in the north and west to major cities during winter [35]. Currently, the Japanese islands have different grid infrastructures, some with very limited transmission capacity, which limits electricity exchange. Hence, grid extensions are required [34,35].

The regions considered for **H_2 imports** are Australia, North America, the Middle East, and South-East Asia [32,34,36]. LNG terminals (both operational and planned) are available in all major urban centres along the coast of JP [37]. The large-scale utilisation of imported H_2 or its derivatives via international supply chains is expected to occur primarily in these coastal areas [29].

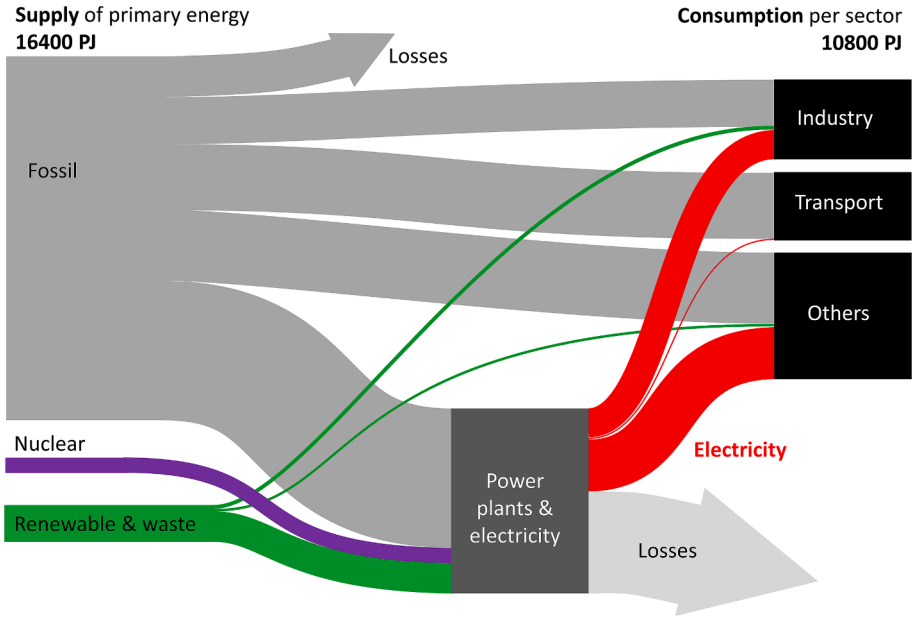

Fig. 2. Sankey diagram illustrating the simplified Japanese energy supply and demand in 2022, created in this study using data from the International Energy Agency (IEA) [27].

3.2. Germany

Fig. 3 shows the **current** total energy flows in terms of supply and consumption for DE in 2022 [27]. All nuclear power plants in DE were shut down in spring 2024 (politically decided phase-out). Compared to the total consumption, H_2 consumption (mostly grey) is currently low in DE at 150 PJ/year (not shown, only approximately 1.7 % of the total demand). H_2 is used in the sectors of basic chemicals (e.g., NH_3 and MeOH) and petrochemicals (production of conventional fuels) [38]. DE produced approximately 2.4 million tonnes of NH_3 in 2021, which corresponds to 45 PJ/year [39]. The total net NH_3 and MeOH imports in DE amounted to approximately 26 PJ/year in 2022 (approximately 0.3 % of the total energy demand) [40]. Historically, DE has not had any LNG terminals, but they have gradually expanded since 2022 due to the Ukraine crisis [39].

The German government has set **interim** targets for the period 2030–2035. GHG emissions are planned to be reduced by 65 % by 2030 compared to 1990 levels (in 2023, they were reduced by approximately 45 % compared to 1990 levels). The government's target is to generate at least 80 % of electricity from renewable energy by 2030. Another goal is to phase coal out by 2038 at the latest. DE aims for an H_2 core network approximately 9700 km in length by 2032. A further objective is to increase the amount of imported H_2 and its derivatives by approximately one order of magnitude to 160–320 PJ/year by 2030 [7,40].

The German government aims to achieve climate neutrality by **2045**. It is estimated that the final energy consumption for a climate-neutral supply in 2045/2050 will decrease by approximately 2000 PJ/year to approximately 7000 PJ/year in the industry, transport, and building sectors, compared to 2022 levels [41,42,43]. Strong electrification is expected with an increase in electricity demand from approximately 2200 PJ/year in 2022 to 4000–4600 PJ/year in 2045 [40,41,43]. The German government expects the total H_2 demand to be approximately 1300–1800 PJ/year by 2045, with an import fraction of >70 % [7,40]. This range is subject to considerable uncertainty, with a total range of 200–2900 PJ/year across different studies in the literature [7,12,18]. In the medium-term, the German government assumes that a large part of the demand for H_2 will be covered by pipelines. An H_2 derivative demand of approximately 700 PJ/year is expected for climate neutrality (e.g., NH_3, LOHC, MeOH, naphtha, and E-fuels).

This demand is expected to be largely met by **imports** from ships. German LNG terminals are expected to be used for this purpose [7]. At the time of writing, German LNG terminals had a maximum capacity of 470 PJ/year and were located at North Sea ports (Brunsbüttel, Stade, and Wilhelmshaven). The utilisation of these three ports (along with further activities in Hamburg and Rostock) is also planned for the import of H_2 derivatives. Several NH_3 projects are currently planned for DE and are expected to be completed before 2030. The German government is also considering the use of MeOH and LOHC; it is currently unclear whether LH_2 is being considered [7]. Within the European network, the ports of Rotterdam and Antwerp also play a major role in H_2 ship imports for DE. Potential countries for the production and export of green H_2 by ship are spreading worldwide. At the time of writing, the following countries were particularly relevant to DE: Australia, South and North America (Argentina, Chile, and Canada), Africa (Namibia and South Africa), India, and the Middle East (Saudi Arabia and the United Arab Emirates) [7,12,18,44,45].

The potential for **renewable** electricity generation from wind and PV is unevenly distributed in DE. Due to the higher annual full load hours, wind energy contributes a considerably larger amount of renewable energy than that of PV. The potential for PV is marginally higher in the south and south-east while the north is more favourable for wind energy. Overall, the greatest potential per unit area for renewable electricity generation from wind and PV is in the north-west, whereas offshore wind potential is greatest in the North Sea [46].

3.3. Country comparison, discussion, and theoretical potential

JP and DE share several similarities in their energy landscape. These include similar total energy demands and end-sector use, low energy self-sufficiency, a significant increase in PV capacity to similar levels, and similar interim and final GHG targets. Both countries focus on closed material cycles and improved energy efficiency. JP and DE also have similar domestic production capacities for grey MeOH, NH_3 and H_2. Additionally, both have similar decarbonisation strategies and targets that rely on H_2 and NH_3 imports [32,47]. Table 1 mainly lists the differences between DE and JP.

A comparative assessment of the differences listed in Table 1 yielded the following observations: JP's energy dependence on imports is greater. Wind power is currently limited in JP and can or cannot be expanded by floating offshore wind energy in the future. The installed PV power is similar, although JP has better conditions. Nuclear energy contributes significantly to the energy mix in JP, but not at all in DE. DE

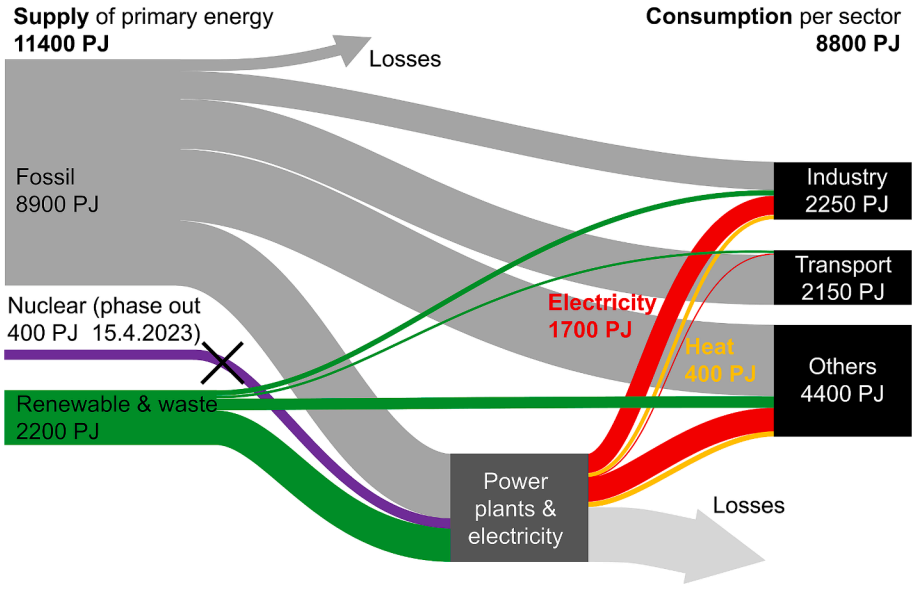

Fig. 3. Sankey diagram illustrating the simplified energy supply and demand for Germany in 2022, created in this study using data from the International Energy Agency (IEA) [27].

Table 1
Differences between the Japanese and German energy systems in relation to the proposed HT-TES-P2H concept. CCS, carbon capture and storage; EU, European Union, LH_2, Liquefied hydrogen; LNG, liquefied natural gas; PV, photovoltaics.

Aspect	Japan (JP)		Germany (DE)
Energy demand [27]	10,800 PJ/year (2022)	>	8800 PJ/year (2022)
Primary energy self-sufficiency ratio [47]	12 % (2019)	<	35 % (2019)
Electricity supply			
Wind installed power [48]	5 GW (2022)	<	66 GW (2022)
Wind Resources	Limited potential in northern and western regions; significant floating offshore potential [34]	<	High potential in north west regions and North Sea [46]
PV installed power [49]	91 GW (2023)	>	82 GW (2023)
PV average practical solar potential [50]	3.45 kWh/kW_p	>	2.96 kWh/kW_p
PV seasonality index [50]	2.05 (smaller seasonality)	<	4.37 (larger seasonality)
Share of nuclear power	20–22 % (2030) [29] ~20 % (2040) [33]	>	Phase out in 2023
International electricity interconnection	Non	<	EU max. export 18 GW, total export 270 PJ/year; import was smaller (2022) [51]
H_2 & H_2 derivative import			
Gas network/distribution & storage [47]	No international gas network; replacement of natural gas by synthetic methane		Planned H_2 core network in the EU and DE; DE plans considerable H_2 import via pipelines; large H_2 storage projected (seasonality in DE)
LNG	Established, more than 50 years ago [47]; e-LNG replaces natural gas in the future		Rapid expansion from 2022 since Ukraine crisis; future port use for H_2 derivative import
NH_3	Also targets for fuel use [30]		Likely H_2 carrier for ports [52]
LH_2	Focus as energy carrier, e.g., Kawasaki Heavy Industries LH_2 ship [14]		Some interest, but limited focus
CCS	Integral part of energy strategy		Historically no focus, recent interest for CO_2 network with neighbouring countries [7]

is integrated into the European electricity and gas grid, whereas JP's supply is isolated. The roles of natural gas and H_2 networks are less important in JP. JP has numerous ports, which serve as international logistics hubs managing 99.6 % of the country's imports and exports. Many power generation plants, as well as steel and chemical industries, are located at the ports. These plants in the port surroundings emit approximately 60 % of JP's CO_2 emissions [29]. As with DE, the Japanese government aims to explicitly expand port infrastructure to introduce large quantities of H_2 and NH_3 [29]. Compared to DE, JP tends to partially view NH_3 and (e)-LNG as fuels rather than as H_2 carriers. Carbon capture and storage (CCS), and consequently the use of C-containing gases, plays a greater role in JP. The development of LH_2 has progressed further in JP. Nevertheless, JP will also likely develop the potential to convert NH_3 into H_2 in port areas (e.g., for steel production, the chemical industry, and power generation).

Generally, when comparing H_2 carriers (LNG, MeOH, LH_2, NH_3, and others), the momentum for the utilisation of NH_3 as a future international navigable H_2 carrier appears to be high in DE, JP, and worldwide [53]. As explained, DE and JP expect a significant increase in imports [54]. Over 120 ports already have NH_3 infrastructure and 10 % of global NH_3 production is already traded [11]. Hence, there is already a deep-sea supply chain for NH_3.

Liquid NH_3 is imported to deep-sea ports by ships. A distinction can be made between large-scale centralised direct use in the port environment or decentralised use with available NH_3 distribution routes (e.g., via trains, trucks, inland waterways for filling stations, or industrial sites) [8,55,56,57,58]. Centralised plants are larger in comparison and are expected to operate continuously. Ships with capacities of several tens of thousands of tonnes of NH_3 [6], as currently available, could then supply NH_3 crackers with a capacity of several thousand tonnes of NH_3 per day. The analysed HT-TES-P2H concept for converting NH_3 into H_2 (Fig. 1) revealed a certain complexity; thus, it is assumed to be more suitable for larger central plants. The required renewable resources for the proposed HT-TES-P2H concept could be available in DE in the north and in JP in the north and west. Another argument in favour of centralised conversion near ports with a high supply of renewable electricity is that lower transport costs can be expected for a steady flow of H_2 via pipelines compared to the transport of volatile wind and PV electricity via power lines [59]. Thus, the direct central reconversion of NH_3 into H_2 using renewable energy and the HT-TES-P2H system near import ports presents significant potential. The H_2 produced can then be used, for example, for gas grid injection, electricity generation, or large-scale industrial processes (e.g., direct iron ore reduction).

The following estimate illustrates the theoretical potential for DE as an example. A heat supply is required to operate the NH_3 crackers (an endothermic process). State-of-the-art (SoA) technology utilises NH_3 directly or indirectly as a fuel. The quantity of NH_3 fuel is determined by the H_2 yield from the NH_3 conversion process. For an effective NH_3 process, approximately 80 % of the NH_3 is converted into H_2, and approximately 20 % is used as fuel (see Subsection 4.3.4 and Section 5). It is expected that approximately 700 PJ/year of the DE total energy consumption of approximately 7000 PJ/year will be imported as H_2 derivatives by 2045 [7]. The maximum theoretical reduction potential for imported NH_3 through the HT-TES-P2H concept is therefore approximately 140 PJ/year (20 % of 700 PJ/year) for DE by 2045. Additionally, a reduction in size of up to 20 % is expected across the entire supply chain. This impact extends to the port infrastructure, shipping capacity, synthesis plants with electrolysis and the installed renewable capacity in the exporting country. Consequently, an NH_3 cracker should be equipped with an HT-TES-P2H system. Additional wind and PV systems would have to be installed in DE; however, these installations would be significantly smaller than the savings from wind and PV installations in the exporting country. A detailed analysis of the economic potential is presented in Subsection 5.4.

4. Results and discussion of technology assessment

4.1. High-temperature thermal energy storage with power-to-heat technologies

Table 2 presents a brief overview of **TES** systems operating in the HT range. Sensible heat storage systems based on solids (ceramics) and liquids (nitrate salt and pressurised water to a certain degree) have been implemented commercially and on larger scales. The solid media ceramic regenerator TES has been used for decades in the iron and steel, as well as glass, industries, with a wide operational temperature range. Molten salt storage TES systems are used in concentrating solar thermal power plants and are currently limited to a maximum temperature of

Table 2
Brief summary of major high temperature (HT) thermal energy storage (TES) technologies [60,61,62,63]. HX, heat exchanger; HTF, heat transfer fluid; R&D, research and technology development.

Typ. storage material	Heat transfer concept	Typical HTF	Typ. temperatures	Market status
Solids				
Shaped ceramic bricks	Direct contract regenerator	Gases (e.g., air, flue gas)	400–1600 °C	Commercial, > 100 MWh
Stones packed bed	Direct contract regenerator	Gases	200–800 °C	Pre-commercial
Ceramic bauxite particles	Two tank concept with HX	Ceramic bauxite particles	400–800 °C	Pre-commercial
Other solids[+]				R&D and pre-commercial
Liquids				
Pressurised water	Sliding pressure/temperature	Press. water, satur. steam	150–230 °C	Commercial up to 30 MWh
Molten nitrate salt	Two tank concept with HX	Superheated steam	170–560 °C	Commercial, > 1000 MWh
Others liquids[*]				R&D and pre-commercial
Phase change				
Solid-liquid nitrate salt	Indirect contact regenerator	Water, steam	130–330 °C	R&D
Solid-liquid metals	Indirect contact regenerator	Gases	> 500 °C	R&D
Thermochemical				
$CaO/Ca(OH)_2$ solid–gas	Indirect contact reactor	Steam	400–600 °C	R&D
Other solid–gas reactions[#]				R&D

[+] Examples include concrete, graphite, steel and sand.
[*] Examples include thermal oil, liquid metal, chloride molten salt, single tank with mixed nitrate salt and solids.
[#] Examples include salt hydrates, hydroxides, hydrides, carbonates and metal oxides.

565 °C. The minimum temperature depends on the solidification temperature of the salt mixture and can be as low as 170 °C. The disadvantages of pressurised water/steam storage tanks (called 'Ruths') are the costly pressure vessel, the limited temperature range, as well as the decreasing pressure and temperature during discharge, limiting their use cases. Other TES principles utilise a solid–liquid phase change material (PCM) and reversible gas–solid reactions. PCM and thermochemical storage (TCS) could be favoured to supply heat closer to the isothermal process demand (e.g., for MeOH and LOHC); however, these two HT-TES technologies are still under development or pre-commercial. Sensible heat storage systems based on molten salt and ceramic regenerators are currently the only HT-TES technologies that have been commercially realised on a large scale. For cost-effective realisation, sensible HT-TES require a greater temperature difference (e.g., > 100 °C). The working temperature range and heat transfer fluids (HTFs) are essential for system integration. Further details on HT-TES can be found in the literature [60–62].

Currently, several technologies are available for **electric heating**. Examples include resistance, dielectrics, induction, radiation, and arc electric heating [64]. Resistance heating bundles are widely used in flow heaters for HTFs, such as gases and molten salt, based on the current SoA. A heating element typically consists of mineral-insulated heating rods. For this mineral-insulated heater type, the maximum HTF temperature is typically limited to approximately 600 °C for long-term continuous operation and based on the typical surface heat flow of the heating elements. Regenerators that use air as HTF typically exhibit a drop in outlet temperature during discharge. However, this technology can also provide a constant process outlet temperature, which can be achieved with a bypass flow and a TES temperature higher than the discharge temperature. Assuming a usable discharge temperature of approximately 50 °C lower than the maximum regenerator TES temperature, along with the P2H 600 °C limitation, results in a similar limit of approximately 550 °C for both solid media and molten salt TES systems, which can currently be realised with SoA technology. However, in principle, this temperature could be increased in the future through research and technology development (R&D) in the fields of P2H and molten salts.

4.2. Overview of chemical energy carriers

Table 3 lists the sea transport options for the four liquid H_2 derivatives and their advantages and disadvantages. A distinction can be made between the two groups: one without carbon (NH_3, LOHC) and one with carbon handling (MeOH, LNG/e-LNG) [3,44]. All climate-neutral options for H_2 carriers with carbon require additional effort for CO_2 handling including the following:

- Carbon capture and utilisation (CCU) with recycling in a closed cycle (e.g., liquid cold CO_2 transport by ship and reutilisation)
- CCS
- Biomass utilisation
- Direct air capture (DAC) technologies
- (Unavoidable CO_2 from industrial processes is typically not considered CO_2-neutral)

One advantage of derivatives with carbon is that they provide an increased amount of H_2 through a reaction with H_2O during reconversion (CH_3OH: 4 H_2 → 6 H_2; CH_4: 4 H_2 → 8 H_2, see Table 3 with and without this reaction and the increased volumetric energy density). However, additional energy must be used to heat and evaporate the water. The energy utilisation rate presented in Table 3 (defined from H_2 via carrier to H_2) includes both energy losses and conversion efficiencies, as determined by Staudt et al. [18]. The low utilisation rates of MeOH and e-LNG are attributed to the DAC assumption. Thus, higher numbers are feasible for other CO_2 approaches.

In terms of market maturity, NH_3, MeOH, and LNG appear more suitable than LH_2 and LOHC [15]. For LNG, MeOH, and NH_3, the order of magnitude of the market price is generally a few 100 $/tonne, with differences due to market price fluctuations, regional price differences, delivery form (liquid or gaseous), and different taxation (e.g., CO_2). Niermann et al. [16] examined seven different substances as H_2 carriers and concluded that MeOH, toluene, and DBT have the highest potential [16]. Tsogt et al. [65] also concluded that DBT has the highest suitability after analysing four different LOHCs. Hence, DBT was selected as the representative LOHC for this study. The price of DBT, as a representative of LOHC, is approximately 4400 $/tonne, with minimal consumption of the carrier (literature indicates a loss of 0.01–0.1 % per full cycle) [11,66].

4.3. Endothermic reconversion process

Niermann et al. [16] pointed out that the provision of the necessary heat for H_2 reconversion is crucial for the efficiency of the overall value chain of chemical carriers. In terms of the cost structure, reconversion also contributes significantly to the overall H_2 costs [53]. Therefore, the efficient reconversion of H_2 derivatives is an important aspect. Fig. 4

Table 3
H_2 carrier options for sea transport, along with their pros and cons. The table was compiled from several sources [3,5,6,7,11,16,17,18,44,45,67,68,69,70,71,72]. TRL, Technology readiness level.

Abbreviation	NH_3	LOHC (DBT)	MeOH	(e)-LNG
Full name	Liquefied Ammonia	Liquid Organic Hydrogen Carrier	Liquid Methanol	Liquefied Methane
Carbon in carrier	No	No	Yes	Yes
Volumetric H_2 content	113 kg-H_2/m³	69 kg-H_2/m³	99 kg-H_2/m³ (148 kg-H_2/m³)$	108 kg-H_2/m³ (215 kg-H_2/m³)$
Product storage parameters	-33 °C @ atm. P (amb.T@10-30 bar)	Ambient Temperature @ atmospheric pressure	Ambient Temperature @ atmospheric pressure	-162 °C @ atmospheric pressure
Large-scale ship boil-off rate [72]	0.02 - 0.04 %/day	No	0.005 %/day	0.012 – 0.12 %/day
Intermediate storage for days	Cold flat bottom tank	Flat bottom tank, large LOHC hold-up	Flat bottom tank	Compression for existing pipelines and caverns
Long-term storage for season	Conversion to H_2 and CH_2 cavern	Conversion to H_2 and CH_2 cavern	Conversion to H_2 and CH_2 cavern	CH_4 cavern
TRL of synthesis from H_2 & charging infrastr.	Haber–Bosch process, known but not yet electrified	No significant installations to date	Pilot scale facilities available	Experience from methanation of coal
Amount of shipping (existing world market)	20 million tonnes/year (190 million tonnes/year)	< 0.01 million tonnes/year, but similar to diesel	30 million tonnes/year (110 million tonnes/year)	370-570 million tonnes/year
TRL of discharging infrastructure to H_2	Similar reactor design as methane-steam reforming	No significant installations to date	No significant installations to date	Large-scale methane-steam reforming known
Likely future direct market (fuel, chemical)	Yes	No	Yes	Yes
Lower heating value (LHV)	5.2 kWh/kg	not applicable	5.5 kWh/kg	13.9 kWh/kg
Hazardous substance properties+	Flammable Cat 2 Health hazard Cat. 3, Environ. hazard Cat 2	Flammable Cat 1, Health hazard Cat 1, Environmental hazard Cat 4	Flammable Cat 2, Health hazard Cat 3	Flammable Cat 1
H_2-H_2 energy utilisation rate [18]	63%	68%	57%	47%
H_2 Reconversion:				
Typical Process param.	400-800 °C, 10-50 bar	270-320 °C,1-2 bar(a)	200-400 °C @ 1-30 bar	500-1100 °C @ 3-25 bar
Typical Catalyst	Ni, Co-Fe, Ru	Pt	Cu, Pd	Ni
Equilibrium reaction of reactor	$NH_{3(g)}$+46 kJ/mol ↔ $0.5N_{2(g)} + 1.5H_{2(g)}$	H18-$DBT_{(l)}$+589 kJ/mol ↔ H0-$DBT_{(l)} + 9H_{2(g)}$	$CH_3OH_{(g)} + H_2O_{(g)}$ +49 kJ/mol ↔ $CO_{2(g)} + 3H_{2(g)}$	$CH_{4(g)} + 2H_2O_{(g)}$+165 kJ/mol ↔ $CO_{2(g)} + 4H_{2(g)}$
Additional Evaporation	+ 23 kJ/mol $NH_{3(l\rightarrow g)}$	non	+ 37 kJ/mol $CH_3OH_{(l\rightarrow g)}$ + 44 kJ/mol $H_2O_{(l\rightarrow g)}$	+ 44 kJ/mol $H_2O_{(l\rightarrow g)}$
Theoretical heat for H_2 reconversion	4.2 kWh/kg-H_2 (6.4 with evaporation)	9.1 kWh/kg-H_2	2.3 kWh/kg-H_2 (6.0 with 2x evaporation)	5.7 kWh/kg-H_2 (8.8 with evaporation)

$= Back-calculated value for additional supplied H_2 due to H_2O reactions.
+ = Hazardous properties due to pressure and cryogenic liquefaction not included; GHS/CLP labelling (EC1272/2008), https://gestis.dguv.de/.

shows the typical process and heat integration with heat sources and sinks for the reconversion of an H_2 carrier to H_2. The H_2 carrier is stored unpressurised (at ambient temperature or below ambient temperature in cold conditions), preheated, and converted to H_2 in an endothermic reactor. The minimum process temperature is determined by the thermochemical equilibrium and kinetic reaction limitations. The maximum process temperature is constrained by factors such as catalyst stability, vapour pressure, structural material/reactor cost, and corrosion.

The heat required for the endothermic reconversion of LOHC, NH_3, LNG, and MeOH is often supplied internally via combustion, utilising the following technical solutions:

1. Combustion of part of the feed gas (NH_3, methane, and MeOH)
2. Combustion of part of the product gas (H_2)
3. Combustion of the off-gas from gas purification
4. Exothermic partial oxidation (POX) of feed gas (NH_3, methane, and MeOH) with O_2

The exothermic POX process can be combined with the decomposition or steam reforming (SR) reactions to form an autothermal (AT) process. AT processes have been considered for three H_2 carriers: NH_3 [73,74], methane [75,76], and MeOH [77]. During the endothermic conversion, an additional (not easily avoidable) off-gas flow with a calorific value is often available (e.g., from pressure swing adsorption (PSA) gas purification), which can also be utilised for combustion. Often, this off-gas flow may not be sufficiently large to supply all the required heat for the endothermic process. All four methods for internal heat supply (combustion of feed, H_2 and off-gas, as well as POX) have the disadvantage of reducing the H_2 yield, which consequently requires a larger amount of H_2 carrier to be imported. The aim of the work presented is to minimise the internal heat supply via combustion and to supply heat externally to achieve a high H_2 yield and low quantity of H_2 carrier import.

The required endothermic heat can also be supplied by an external source, such as electrical power, waste heat from industrial processes, or a climate-neutral gas [73,78]. However, the latter two methods are often unavailable. Direct utilisation of electricity is disadvantageous because renewable electricity is not always available. Hence, this work pursued

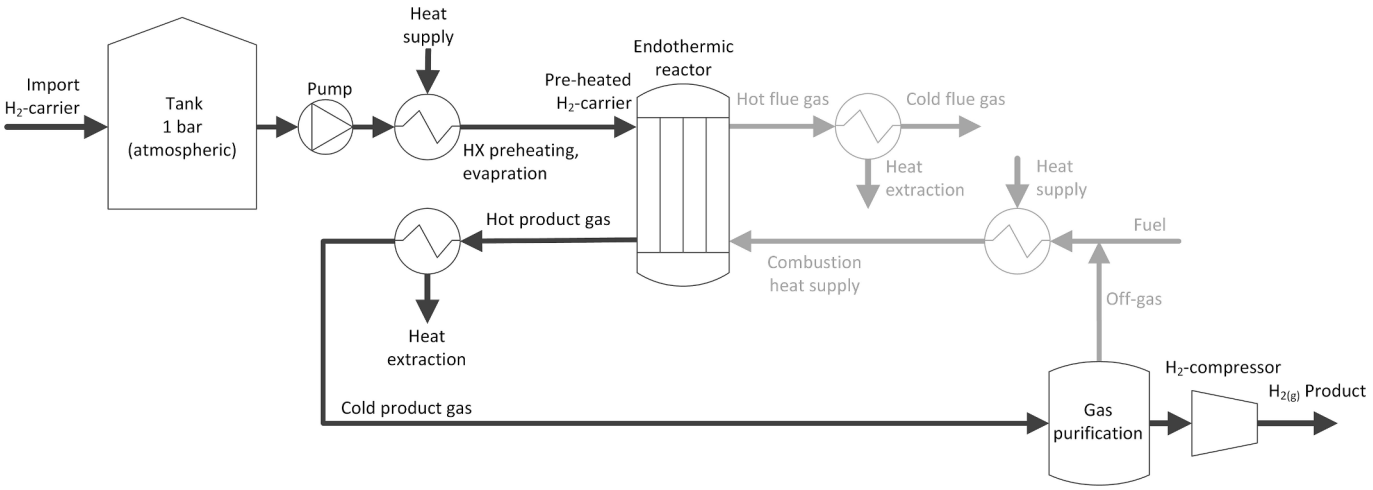

Fig. 4. Simplified scheme illustrating the endothermic conversion of H_2 carrier to H_2. The illustration was abstracted and summarised from the four individual technologies – LOHC, NH_3, LNG, and MeOH – as part of this work.

the approach of converting volatile renewable electricity into HT heat via P2H, storing the heat through a TES, and making it continuously available for the endothermic process.

One technology already being used for smaller applications is the membrane reactor that separates H_2 directly in the reactor using an H_2-permeable membrane (e.g., LOHC [79], MeOH [55,80], methane [81], and NH_3 [74,82,83,84]) [85]. Membrane reactors are promising because they avoid off-gas generation and allow for an increase in external heat integration. Nevertheless, this study focuses on large-scale SoA implementation. Hence, membrane reactors were not considered further in this study.

Some H_2 reconversion systems also incorporate additional steam systems for heat integration and electricity generation from waste heat. The focus of the following detailed discussion of the four H_2 carriers (LOHC, MeOH, methane, and NH_3) is on efficient heat integration, with steam utilisation considered only in selected cases.

4.3.1. LOHC and the reconversion process

The selected LOHC was the conversion between dibenzyl toluene, $C_{21}H_{20}$ (H0-DBT), and the hydrogenated form perhydrodibenzyl toluene, $C_{21}H_{38}$ (H18-DBT):

$$H_{(18)}DBT_{(l)} + 9{\cdot}65\ kJ/mol \leftrightarrow H_{(0)}DBT_{(l)} + 9H_{2(g)} \quad (1)$$

DBT is known for its application as an HTF up to 350 °C [79]. **Advantages** include the simple storage and transport of H0-DBT and H18-DBT in liquid form, using conventional means of transport at ambient temperature and ambient pressure. Furthermore, charging and discharging occur at moderate temperatures (see Table 3), and the flammability and toxicity are relatively low. Although carbon is contained in the carrier medium itself, no CO_2 handling is required during H_2 charging or discharging [65]. A major **disadvantage** is the limited market maturity and penetration. Further disadvantages include the relatively high price (although it is not consumed, it must be kept in stock for H_2 storage over a longer duration), low H_2 volumetric energy density, which is relevant for ship transport, environmental toxicity, the typically employed expensive Pt catalysts, and a large amount of heat required for endothermic reconversion (Table 3).

Approximately 25 % of the energy content of the H_2 produced must be provided for the **dehydrogenation heat** [16]. The typical temperature and pressure range for DBT dehydrogenation is 270–320 °C and 1–2 bar(abs), respectively [16,66,86]. Dehydrogenation occurs within a narrow temperature window and is limited at LTs by thermodynamic equilibrium and at HTs by the DBT vapour pressure [87]. The literature reports specific heat consumption values in a range of 11–12 kWh/kg-H_2 while the theoretical value calculated in this study is 9.1 kWh/kg-H_2 (Table 3) [18,88].

Heat integration in the H_2 reconversion of DBT has been investigated in several studies. An overview by Li et al. [89] highlights research on integration in the areas of fuel cells, cement plants, methanisation, power generation, combined heat and power generation, and road vehicles. Tsogt et al. [65] conducted a multi-criteria analysis of four LOHCs and concluded that DBT has high potential. Heat integration with pinch analysis was also performed for both hydrogenation and dehydrogenation. Runge et al. [66] mentioned the use of P2H and molten salt TES without providing further details as options for the heat supply. Only limited literature is available on the process and heat integration of DBT dehydrogenation.

Based on the information from Li et al. [89] and Niermann et al. [16], the process and heat integration concept shown in Fig. 5 was developed as part of this study.

The TES systems described in Section 4.1 could be integrated to supply the nearly isothermal process heat. It is concluded here that these two basic variants can be distinguished:

1) For sensible TES, heat from the air or molten salt flow (e.g., between 300 and 500 °C) would be introduced into the LOHC reactor via indirect contact (e.g., tube register to separate LOHC and HTF). Air or molten salt would be supplied from the TES-P2H system. Air integration is similar to the utilisation of combustion flue gas, which has already been considered [65]. In the case of molten salts, it is necessary to determine whether unwanted DBT overheating occurs.
2) For PCM or TCS storage systems, which often operate isothermally, the discharge temperature would be adjusted to the LOHC reactor temperature with an additional temperature gradient for heat transfer (e.g., 310 °C). The DBT itself could serve as an HTF (with a high mass flow and small inlet-to-outlet temperature differences, for example, in cross-flow) while the PCM or TCS system could be positioned externally to the LOHC reactor. Alternatively, the PCM or TCS system could be integrated directly into the LOHC reactor. However, in this case, the TES size cannot be scaled independently of the LOHC reactor and may be limited in terms of size and storage duration.

The choice of the TES heat integration concept also depends on the maturity of TES-P2H technology, LOHC reactor size, and TES storage duration. For example, external sensible TES is suitable for large systems, whereas integrated TCS or PCM systems are suitable for small systems with short storage durations.

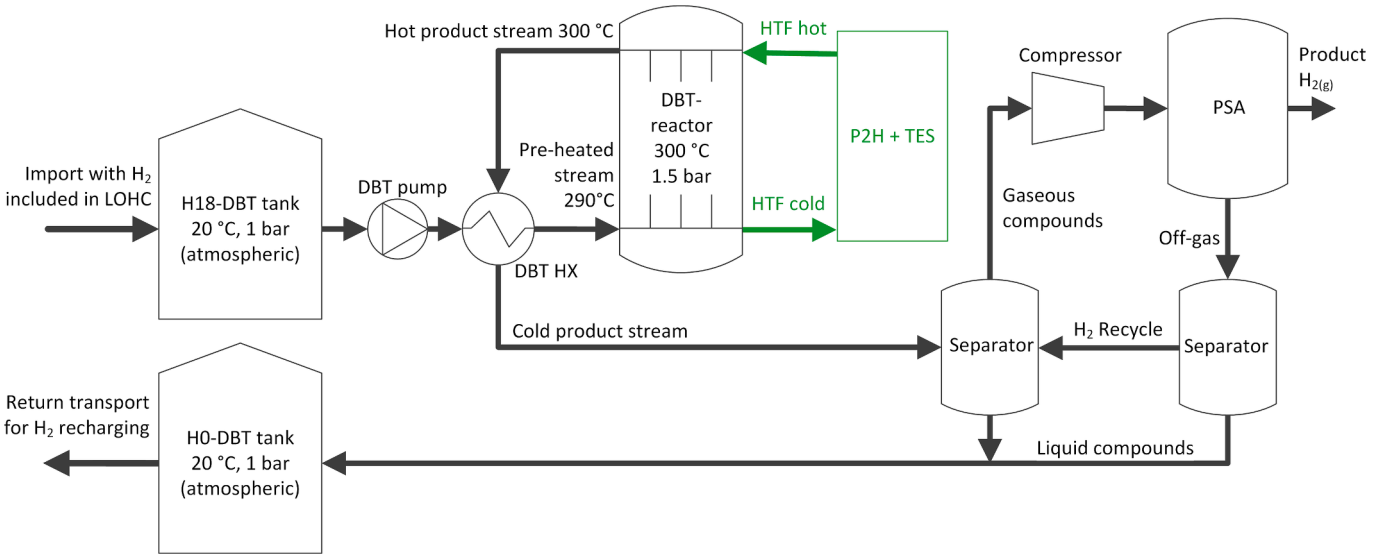

Fig. 5. Simplified scheme illustrating heat and process integration with P2H and TES for DBT as an H_2 carrier. The illustration was created from literature sources [16,89] as part of this study. DBT, dibenzyl toluene; PSA, pressure swing adsorption; P2H, Power-to-heat; TES, thermal energy storage.

4.3.2. Methanol and the reconversion process

The **advantages** of MeOH as an H_2 carrier include simple storage and transport in liquid form using conventional means of transport at ambient temperature and ambient pressure. Additionally, it benefits from existing global trade with known infrastructure, biodegradability, and market potential both as a chemical product and fuel. This enables LT reconversion and has a low reaction heat for H_2 reconversion. However, the low reaction heat cannot be considered in isolation, because a significant amount of additional energy is required for the evaporation of water and MeOH. A major **disadvantage** is the additional effort needed for CO_2 handling, which requires the provision of CO_2 for synthesis and the release of CO_2 during H_2 reconversion (see discussion in Subsection 4.2). There is limited research and industrial activity on the endothermic H_2 reconversion of MeOH compared to other H_2 carriers, as the focus of MeOH is more on direct utilisation as a chemical or fuel [90].

Industrially, H_2 is obtained from MeOH via thermochemical reactions using heterogeneous catalysts [75,77,80,91]. Other concepts exist, but are not considered in this study: homogenous catalysts [92], photocatalysis, aqueous phase reforming [80], electrochemical processes [91], membranes as replacements for traditional reformer-type reactors [80,93], and AT reforming combining POX and SR [77].

Three major reactions are involved in the large-scale reformer-type thermochemical conversion of MeOH into H_2. They are the endothermic MeOH SR (Eq. (2)), and the endothermic MeOH decomposition (Eq. (3)) combined with the exothermic water gas shift (WGS) reaction and (Eq.

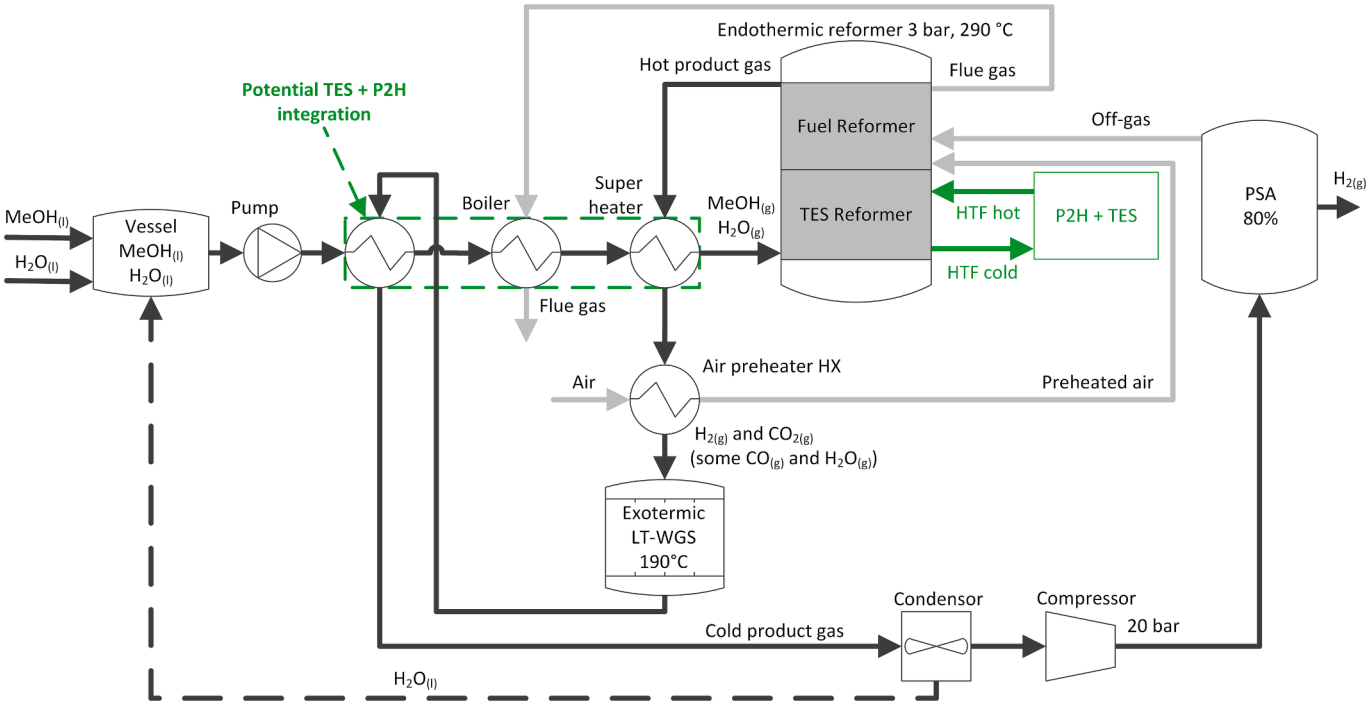

Fig. 6. Simplified scheme of the heat and process integration with P2H and TES for MeOH reconversion. The illustration was adapted from literature sources [75,77,94] as part of this work. LT, low-temperature; P2H, power-to-heat; PSA, pressure swing adsorption; TES, thermal energy storage.

(4))

$$CH_3OH_{(g)} + H_2O_{(g)} + 51\ \text{kJ/mol} \leftrightarrow CO_{2(g)} + 3H_{2(g)} \quad (2)$$

$$CH_3OH_{(g)} + 92\ \text{kJ/mol} \leftrightarrow CO_{(g)} + 2H_{2(g)} \quad (3)$$

$$CO_{(g)} + H_2O_{(g)} \leftrightarrow CO_{2(g)} + H_{2(g)} + 41\ \text{kJ/mol} \quad (4)$$

Eqs. (3) and (4) lead to the same overall MeOH SR reaction (Eq. (2)). In the MeOH to H_2 conversion, there is no clear separation between SR and decomposition with WGS and all three reactions occur [68,75,77,81]. Different reaction mechanisms have been proposed by multiple researchers [58,77,80]. Literature values for the specific heat consumption are in the 10–15 kWh/kg-H_2 range [18,88], which can be compared to the theoretical heat demand of 6 kWh/kg-H_2 for the reactions and evaporation of MeOH and H_2O.

Fig. 6 shows the scheme of the typical **heat and process integration** of a large-scale endothermic MeOH SR unit with an additional LT exothermic WGS reactor [75,77,94]. H_2O and MeOH are miscible and are preheated, evaporated, and superheated together. Hot H_2O-MeOH gas enters the MeOH SR reactor. The MeOH SR reactor is heated by combustion heat (off-gas and possibly additional fuel) and, of interest here, by HT heat from a TES-P2H system. A wide operating parameter range of the MeOH SR reactors can be found in the literature: 150–450 °C and 1–30 bar. Among the two typical catalysts, Pd- and Cu-based, Cu is favoured for large-scale implementation [18,58,75,77,80]. In principle, there are various options for integrating heat from the hot flue gas and hot product gas. The heat integration, as well as the operating temperatures and pressures, were obtained from Papadias et al. [58] in Fig. 6, and the TES-P2H system was added. Remaining CO after the MeOH SR reactor is converted by the exothermic LT WGS reactor into CO_2 and improves the H_2 yield. In the subsequent PSA gas purification, off-gas is produced and combusted. Additional CO_2 separation may also be included (not shown in Fig. 6).

Compared to LOHC, the overall heat integration of MeOH is more complex (e.g., additional H_2O and MeOH evaporators and two reactors instead of one). A relatively large amount of heat is required for the evaporation of water and MeOH (4.6 kWh/kg-H_2). If sufficient heat is not available via the hot product gas flow and hot flue gas, heat for the evaporation of water and MeOH can also be provided by the TES-P2H system. The endothermic reactor temperatures are similar to those of LOHCs; therefore, the TES-P2H technology options do not differ between LOHC and MeOH. Hence, the reader is referred to Subsection 4.3.1.

4.3.3. Methane and the reconversion process

LNG offers **advantages** in terms of high volumetric energy density, already widespread installed infrastructure, and existing technologies for the transport, storage and conversion of LNG and natural gas. Additionally, LNG has favourable properties as both a fuel and a chemical precursor. One of the primary **disadvantages** is the presence of carbon, which requires additional handling of CO_2 during synthesis and H_2 reconversion. A closed CO_2 cycle, involving the shipment of LNG in one direction and liquid CO_2 in the other by ship has been proposed [18,95]. Other disadvantages include liquefaction at LTs (high energy requirements and boil-off), high reconversion process temperatures, and a high amount of energy for H_2 reconversion.

Reformer-type natural gas SR is currently the most widely used method for H_2 production from natural gas. Three major reactions occur. These are the endothermic direct methane SR (Eq. (5)) and the endothermic methane SR with CO production (Eq. (6)):

$$CH_{4(g)} + 2H_2O_{(g)} + 165\ \text{kJ/mol} \leftrightarrow CO_{2(g)} + 4H_{2(g)} \quad (5)$$

$$CH_{4(g)} + H_2O_{(g)} + 206\ \text{kJ/mol} \leftrightarrow CO_{(g)} + 3H_{2(g)} \quad (6)$$

Eq. (6), combined with the exothermic WGS reaction (Eq. (4)), leads to the same overall direct methane SR reaction (Eq. (5)). In the methane to H_2 conversion, there is no clear separation between the direct SR and SR with the WGS, and all three reactions occur. Other methane-to-H_2 conversion developments exist, but are not considered here, e.g., LT (400–550 °C) SR technology, direct thermal decomposition of methane to carbon, and membrane reactors [75,76,96]. A typical literature value for the specific heat consumption is 17 kWh/kg-H_2, which can be compared to theoretical values of 5.7 kWh/kg-H_2 without water evaporation and 8.8 kWh/kg-H_2 with water evaporation [18,97].

Fig. 7 shows the scheme of the typical heat and process integration of a large-scale methane SR unit with a LT WGS reactor [75,94]. The proposed TES-P2H system is additionally presented. LNG and H_2O are evaporated and preheated separately using heat from the ambient environment, hot product gas, and hot flue gas. LNG and H_2O are mixed and enter the endothermic methane SR reactor. The methane SR reactor is heated via combustion heat (off-gas and additional fuel) and, of interest here, by HT heat from a TES-P2H system. A wide operating parameter range for the methane SR reactor can be found in the literature, with values of 500–1100 °C and 3–25 bar. Ni-based catalysts have been mainly used in large-scale SR. The remaining CO in the product gas stream after methane SR is converted in the exothermic WGS reactor. In subsequent PSA gas purification, off-gas is produced and combusted. Additional CO_2 separation may also be integrated (not shown) [75,94].

The electrification of methane SR has been the subject of several scientific studies [98] and industrial developments [99]. However, this electrification is related to direct electrification and does not include the proposed HT-TES-P2H concept, which uses a continuous heat supply to the process from a TES. Several studies have been conducted on methane SR with TES. This refers to SoA nitrate molten salt storage tanks, which can operate at up to 560 °C for the heat supply to membrane reactors for methane SR [100,101]. Traditional methane SR plants operate at higher temperatures (e.g., 520–850 °C; see Fig. 7). This makes the integration of large amounts of heat from the TES-P2H system difficult. Although a solid media regenerator-type TES system is commercially available up to temperatures exceeding 1000 °C, SoA P2H technology is currently limited in temperature to approximately 600 °C (see Subsection 4.1). Hence, R&D efforts for P2H and molten salt systems at elevated temperatures are required to couple larger heat fractions into the reformer. Alternatively, membrane reactors can be used at lower temperatures if scaled up at attractive costs. Another potential application for a TES-P2H system to increase the H_2 yield could be water preheating and evaporation, when there is insufficient heat available from the hot product gas or hot flue gas streams (Fig. 7).

4.3.4. Ammonia and the cracking process

As for the other H_2 carriers (LOHC, MeOH, and LNG), the SoA in science and technology regarding the process and heat integration of endothermic NH_3 to H_2 reconversion was analysed. As NH_3 was selected for further consideration, an in-depth assessment is presented in this subsection. The integration of the TES-P2H system is discussed in Section 5, along with the Ebsilon modelling.

Several reviews and overview articles have been published on NH_3 crackers [55,56,73,74,78,102–108], with a focus on catalyst development [74,82,102,104,105,107,109,110] and some work on numerical simulations [111]. The following discussion summarises the status of the technological development. The synthesis of NH_3 using the Haber-Bosch process from N_2 and H_2 is the world's standard process for NH_3 production (approximately 400–600°C and 100–400 bar). The reverse process of NH_3 cracking has thus far less been commercially used (restricted to a few niche applications). These processes are not optimised for pure H_2 supply and include industrial processes, alkaline fuel cell supplies (only at a smaller scale, maximum ~1 t-H_2/day), and deuterated NH_3 crackers for heavy water production [67,73,74,104].

The following NH_3 cracking reaction is thermodynamically favoured at HT and low pressure:

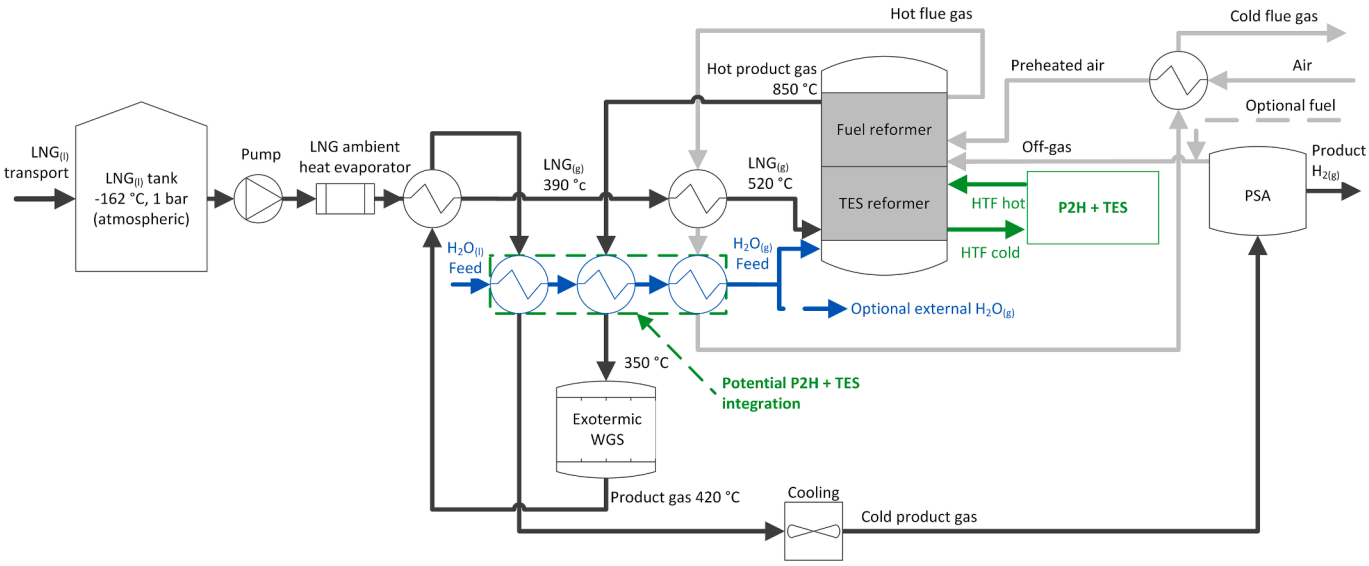

Fig. 7. Simplified scheme illustrating the heat and process integration with power-to-heat (P2H) and thermal energy storage (TES) for LNG-to-H_2 reconversion, incorporating a large-scale methane steam reforming (SR) unit with a low-temperature (LT) water gas shift (WGS) reactor. The illustration was adapted from literature sources [75,94] as part of this research. PSA, pressure swing adsorption.

$$NH_{3(g)} + 46\ \text{kJ/mol} \leftrightarrow 0.5N_{2(g)} + 1.5H_{2(g)} \quad (7)$$

Theoretically, reactors operating at ambient **pressure** are advantageous [105]. However, it is becoming apparent from technological development that higher operating pressures are more favourable (e.g., avoidance of gas compression after NH_3 crackers and more compact design) [56,104,105]. The typical operating pressure should match that of the downstream processes (e.g., PSA 10–40 bar). At higher operating pressures, the thermochemical equilibrium shifts to a lower NH_3 conversion rate. The thermochemical equilibrium data are generally well-known. The conversion rate of the developed catalysts is often determined at atmospheric pressure [67,105]. Busse et al. [112] presented lab-scale measurements of a Ni-based catalyst in the range 450–680 °C and 1–50 bar, demonstrating high conversion rates. To achieve the same conversion (e.g., 95 %) with a pressure increase from 1 to 50 bar, the measurements show that the temperature must be increased by approximately 100 °C. [112]. The reaction enthalpy of 46 kJ/mol applies under standard conditions (25 °C, atmospheric pressure) and increases to 53 kJ/mol at 500 °C (the pressure dependency up to 100 bar is low at 500 °C) [67].

The total **operating temperature** range of the cracking process, as reported in the literature, is 400–1000 °C. The reaction is also kinetically limited (particularly in the lower temperature range). Catalysts can be used to improve the kinetics of the reaction, lower the reaction temperatures, and enhance the conversion rates of the NH_3 cracking process [56,102]. Historically, there have been two temperature windows with long-term experience for NH_3 cracking: 400–500 °C (Ru-based catalysts) and 700–1000 °C (Ni-based catalysts) [78,110,113]. Recently, Ni-based catalysts have also achieved good conversion at moderate temperatures in the range of 500–700 °C [110,112,113]. Additionally, Haldor Topsøe uses a Co-Fe-based catalyst for the intermediate temperature range of 400–800 °C [114,115]. There are arguments for both lower and higher operating temperatures:

- **Benefits and arguments for lower temperatures include**: optimised cracking (pre-cracking and simpler NH_3 post-purification of the hot product gas stream), the use of inexpensive structural materials, such as tubes (e.g., typical steel alloys lose considerable strength above 550 °C), lower heat losses, reduced thermal degradation of the catalyst, and simpler integration of an external heat source.
- **Benefits and arguments for higher temperatures include**: higher conversion rates (with fewer kinetic limitations), higher feasible operation pressures, higher heat transfer rates, and a more compact design.

NH_3 crackers are currently being developed specifically for H_2 production, and are already commercially available, although the technology is still in its pilot phase. Development focuses on catalyst development (e.g., Johnson Matthey, Clariant Catalysts, Haldor Topsøe, and Evonik Catalysts), optimisation of operating parameters (especially pressure and temperature), reactor development, gas separation, and H_2 purification, as well as process integration to improve H_2 yield, energy efficiency, and scalability. In addition to other predominantly non-commercial NH_3-to-H_2 conversion methods with a low technology readiness level (TRL) [73,74,102], several major lines of thermocatalytic reactors are currently undergoing commercial development [56,73,78,84,104,105,114]:

- Reactor designs similar to those used in conventional fired steam methane reforming – **large-scale reformer-type NH_3 cracker:** Companies include Haldor Topsøe, KBR, Thyssenkrupp Uhde, Air Liquide, and Casale. These typically use nickel-based and, to some extent, iron-cobalt-based catalysts, with maximum temperatures of 600–1000°C. These reactors are intended for centralised cracker solutions and have a higher TRL, with some smaller-scale commercial installations [73,104,114,116].
- **Small-scale reformer-type NH_3 cracker:** Often uses (expensive) ruthenium-based catalysts at temperatures of 400–500 °C. These are intended for decentralised NH_3 crackers, with some commercial installations [78,102,103,104]
- **Thermocatalytic membrane reactors:** Companies include H2SITE, Engie, Siemens Energy, and the Australian research institute CSIRO. They often use ruthenium-based (expensive) catalysts at 400–550 °C in combination with an H_2-permeable membrane (based on palladium), offering the advantage of direct N_2 separation. These reactors are small-scale for decentralised NH_3 crackers and have a lower TRL [73,102,104,117].

The separation of mixed gases to obtain purified H_2 fuel can present a challenge. **Removal of N_2 from H_2 and purification of H_2** can be achieved though methods such as adsorption, especially PSA, membrane

Table 4
Concepts for process and heat integration in large-scale reformer-type NH_3 cracker.

Aspect	Industrial development	Scientific literature
NH_3 cracker operating parameters and catalyst	30–50 bar, Co-Fe catalyst, 400–800 °C [114,119] 30–40 bar with Ni-based catalyst [116] 600–900 °C at 20–40 bar [127]; > 40 bar [128] approximately 600 °C and in a single pass [129]	800 °C at 20 bar, Ni catalyst [58] 400–550 °C at 10–30 bar, Ru catalyst [117] 900 °C, 30 bar, Ni catalyst [121] 700 °C at 1 bar, Ni catalyst [122] 500–850 °C, 2 bar [124]
Source of heat supply for NH_3 evaporator	Yes, unknown (flue gas or hot prod. gas) [116] Hot product gas [119] Hot product gas → Steam [120]	Comb. flue gas [8,117] Hot product gas [58,121] Ext. process (turbine flue gas) [122] Ambient heat [124]
Source of heat supply for NH_3 preheater	Yes, unknown (flue gas or hot prod. gas) [116] Flue gas [119] Product and flue gas [120]	Comb. flue gas [8,58,117,122] Hot product gas [121,124]
Source of heat supply for NH_3 pre-cracker	Yes, unknown (flue gas or hot prod. gas) [116] Flue gas [119,120]	No pre-cracker [8,58,117,121,124] possibly, with comb. flue gas [122]
Source of heat supply for NH_3 cracker	Comb. of PSA off-gas + opt. H_2/N_2 [116] Comb. PSA off-gas + H_2,H_2/N_2 or ext. fuel [119] Comb. of PSA off-gas + NH_3 or ext. fuel [120]	H_2O/NH_3 absorption / distillation [8,117] Comb. of PSA off-gas & natural gas [58] Comb. of PSA off-gas and NH_3 [121] Comb. of $N_2 + H_2$ [122] Comb. of PSA off-gas and H_2 [124]
Sources of heat supply and combustion air preheating	Unknown [116,119,120]	Comb. flue gas [8,117,121] Hot product gas [58] Ext. process (turbine flue gas) [122] Unknown [124]
Integration of steam cycle in combustion flue gas	Yes, integration unknown [114] No or unknown [116,130] Yes, used for NH_3 evaporator [120] Yes, steam export [128]	Steam turbine [8,117] No [121,122] No, but gas turbine in comb. flue gas [124]
NH_3 separation	Yes, but unnamed [114] H_2O/NH_3 absorption / distillation [116,128]	8 vol% NH_3 in product gas, H_2O/NH_3 absorption / distillation 8 stages [8,117] Yes, but unnamed [121] No, direct 99 % N_2-H_2 usage [122] No [124]
N_2 separation (efficiency)	PSA (unknown) [114,116,128]	Cryogenic cycle [8,117] PSA (unknown) [121] No, direct N_2-H_2 usage [122] PSA (75 %) [58,124]
NH_3 delivery quantities	15–500 t-H_2/day [114,115,119] 10–1200 t-H_2/day [116] 5–1300 t-H_2/day [128] 70–700 t-H_2/day [131]	200 t-H_2/day [8,117] 50–350 t-H_2/day [58] 34 t-H_2/day [121] 106 t-H_2/day [122] 420 t-H_2/day [124]

separation, LT separation (e.g., cryogenic distillation), and metal hydride separation. PSA is established for larger-scale industrial applications (typically 10–40 bar, with H_2 recovery rates of 65–90 %) [81]. Studies on cryogenic distillation for higher H_2 purities and higher recovery rates have also been reported [105]. Membrane technology has emerged as an alternative [81,118]. There are several techniques for **removing the remaining NH_3 from syngas**, including thermal incineration (which produces nitrogen oxides (NO_x)), scrubbing (which produces wastewater), the catalytic method (which uses an additional catalyst at temperatures exceeding 650 °C with lower energy efficiency), and thermally regenerated adsorbers [102,105]. Due to differences in the H_2 characteristics and conditions, a combination of technologies (PSA and cryogenic distillation) or a steam-washing scrubber may be required.

In thermocatalytic reactors, the H_2 derivative is preheated and fed through a reactor loaded with a catalyst. Various aspects must be considered during **process integration**. These include the evaporation and preheating of NH_3, the design of the cracker for H_2 production, H_2 separation and purification of the process gas (e.g., N_2, CO_2, and the remaining NH_3), gas expansion and compression, if necessary, and the provision and integration of heat [58,78,84,114,116,119,120]. Heating often occurs via combustion (e.g., NH_3 itself, in combination with N_2-H_2 off-gas from the PSA, or with the injection of O_2 and using POX for NH_3 AT operation). Electrically heated crackers are also being developed and are commonly used on smaller scales. The required H_2 purity depends on the application. For example, lower purity requirements must be met when feeding H_2 into the gas grid or for industrial supply (e.g., 99.9 %) compared to H_2 supply for refuelling stations (99.97 % ISO 14687:2019) or proton exchange membrane (PEM) fuel cells (maximum 0.1 ppm NH_3) [105,121].

Table 4 summarises the concepts of heat and process integration for large-scale reformer type NH_3 crackers (large-scale membrane reactors [84] and small-scale units, such as those listed in Cha et al. [103], are not included here). Several large-scale NH_3 crackers have been simulated as complete systems in scientific studies, with the Aspen software commonly used. Jackson et al. [8] and Makhloufi and Kezibri [117] modelled an NH_3 cracker system for centralised H_2 supply to filling stations and industry. Restelli et al. [121] modelled the long distance NH_3 value chain from synthesis to cracking and a centralised cracker with a Gibbs reactor. Papadias et al. [58] compared different H_2 carriers in terms of production, transmission, decomposition, and storage. For the NH_3 cracking unit, a flow diagram and performance model were developed. Cesaro et al. [122] examined NH_3 cracking for large-scale power plants. Pashchenko and Mustafin [123] modelled and examined the heat integration of the NH_3 cracker in detail. The NEDO-WE-NET study utilised ambient heat for NH_3 evaporation and contains details

on the mass flow, flow composition, temperature, and pressure; therefore, it was used for model validation in this study (see Subsection 5.1) [124,125]. In the literature, the energy consumption of NH_3 crackers is reported over a wide range of 4.3–16 kWh/kg-H_2, with most data in the range 8–12 kWh/kg-H_2. The theoretical value for cracking is 4.3 kWh/kg-H_2, and cracking with evaporation results in 6.4 kWh/kg-H_2 (Table 3) [11,18,88,104].

The summary of **industrial commercial development** presented in Table 4 demonstrates that high pressures in NH_3 crackers (20–50 bar) are favourable for large-scale implementation. It can be assumed that these pressures were selected to match the PSA pressure to avoid additional gas compression stages. Limited information has been published on the maximum temperature level of the NH_3 catalyst in the crackers under commercial development; therefore, a wider range of 400–900 °C is possible. The frequent use of NH_3/H_2O absorption/distillation suggests that the cracker is designed with a residual amount of NH_3 in the hot product gas stream, which occurs at lower operating temperatures. PSA is widely used for further purification (compared to cryogenic purification as the other commercial alternative). Heat integration is a widely used method. The heat sinks include the NH_3 evaporator, NH_3 preheater, NH_3 (pre)crackers, as well as combustion air and fuel preheating. The heat sources include the hot product gas and hot flue gas streams (from NH_3, H_2, $H_2 + N_2$ off-gas, and external gases). Industrial developments typically report energy efficiencies rather than specific heat consumption in kWh/kg-H_2. Energy efficiencies can be difficult to interpret (see the efficiency discussion in Section 5). A typical value for H_2 yield in industrial developments is 78 %, using heat supply from NH_3 [115,116,126].

5. Results and discussion of technical heat integration

Compared to other H_2 derivatives, the NH_3 pathway has no significant obstacles (Table 3). NH_3 is supported by energy policies in DE and JP, and existing supply chains can be utilised for its distribution. The commercial-scale reconversion of NH_3 into H_2 has not yet been established. The energy required for the endothermic reconversion of NH_3 to H_2 is typically supplied via NH_3 combustion. This leads to a larger (undesirable) fraction of valuable NH_3 imports. For this reason, heat integration with an external heat supply for NH_3 crackers is analysed in more detail through simulations in the following subsections.

First, efficiencies and specific energy consumptions were defined to evaluate the results. The H_2 yield, η_{H2}, is generally defined for the four considered H_2 carriers as the ratio of the molar flow of the H_2 product to the molar flow, F, of the chemical carrier, multiplied by the stoichiometric coefficient, X, of the equilibrium equations (see also Table 3):

$$\eta_{H2} = \frac{F_{H_2}^{product}}{X \cdot F_{Carrier}^{feed}} \tag{8}$$

The H_2 yield for NH_3, $\eta_{H2,NH3}$, is defined in terms of the mass flow, $\dot{m}$, of H_2 as the product gas and NH_3 as the feed gas, where M represents the molar mass of H_2 and NH_3. According to this definition, $\dot{m}_{NH_3}^{feed}$ includes both the NH_3 used for H_2 conversion and the NH_3 used as fuel:

$$\eta_{H2,NH3} = \frac{\dot{m}_{H_2}^{product}}{\frac{1.5 \cdot M_{H2}}{M_{NH3}} \dot{m}_{NH_3}^{feed}} = \frac{\dot{m}_{H_2}^{product}}{\frac{1.5 \cdot M_{H2}}{M_{NH3}} \left(\dot{m}_{NH_3 \rightarrow H_2}^{feed} + \dot{m}_{NH_3,heat}^{feed} \right)} \tag{9}$$

Certain studies defined the NH_3 energy efficiency, $\eta_{E,NH3}$, where H_{LHV} are the LHVs of H_2 and NH_3 [115,116,129]:

$$\eta_{E,NH3} = \frac{\dot{m}_{H_2}^{product} \cdot H_{H_2,LHV}}{\dot{m}_{NH_3}^{feed} \cdot H_{NH_3,LHV}} \tag{10}$$

The total NH_3 energy efficiency, $\eta_{E,total}$, includes external TES heat and the electricity consumption of the key electrical components, such as pumps and compressors:

$$\eta_{E,total} = \frac{\dot{m}_{H_2}^{product} \cdot H_{H_2,LHV}}{\dot{m}_{NH_3}^{feed} \cdot H_{NH_3,LHV} + P_{el} + \dot{Q}_{TES}} \tag{11}$$

Notably, this definition of $\eta_{E,total}$ does not include the additionally considered ambient heat flow, $\dot{Q}_{amb}$, used in some cases, as it is assumed to be freely available.

Inserting Eq. (9) into Eq. (10) leads to the following:

$$\eta_{E,NH3} = \eta_{H2,NH3} \frac{1.5 \cdot M_{H2}}{M_{NH3}} \cdot \frac{H_{H_2,LHV}}{H_{NH_3,LHV}} = \eta_{H2,NH3} \cdot 1.134 \tag{12}$$

When H_{LHV} values are inserted into Eq. (12), it becomes evident that this definition leads to an impractical energy efficiency, yielding values of $\eta_{E,NH3} > 100$ % for $\eta_{H2,NH3} = 1$. Therefore, only the energy efficiency, $\eta_{E,total}$, as defined in Eq. (11) was used for the Sankey diagram (Fig. 12). To determine the differences between the following modelling cases, several specific energy consumptions were defined as the energy required per unit mass of produced H_2 (kWh/kg-H_2). Using mathematical conversion of Eq. (9) and the LHV of NH_3, the specific NH_3 heat consumption, $h_{NH3,heat}$, can be calculated:

$$h_{NH3,heat} = \frac{M_{NH3}}{1.5 \cdot M_{H2}} \left(\frac{1}{\eta_{H2,NH3}} - 1 \right) H_{NH_3,LHV} \tag{13}$$

For example, an H_2 yield of $\eta_{H2,NH3} = 80$ % results in $h_{NH3,heat} = 7.3$ kWh/kg-H_2. This value can be compared to the theoretical energy required for NH_3 cracking, which is 4.2 kWh/kg-H_2, and the theoretical energy required for NH_3 evaporation and cracking, which is 6.4 kWh/kg-H_2 (Table 3). Eq. (13) shows that if all NH_3 feed gas is converted into H_2 ($\eta_{H2,NH3} = 1$), the specific NH_3 heat consumption, $h_{NH3,heat}$, becomes 0. This occurs when all the heat is supplied externally.

In this study, the two external heat sources – ambient heat and HT heat from an HT-TES-P2H system – were analysed. The specific heat from the HT-TES-P2H system is defined as the quotient of the heat flow from the HT-TES-P2H system to the product mass flow of H_2 (kg/s):

$$h_{\dot{Q},TES} = \frac{\dot{Q}_{TES}}{\dot{m}_{H_2}^{product}} \tag{14}$$

Similarly, the specific heat from the ambient environment is defined as:

$$h_{\dot{Q},amb} = \frac{\dot{Q}_{amb}}{\dot{m}_{H_2}^{product}} \tag{15}$$

Analogous to the external heat, the specific electricity consumption, h_{Pel}, of the main electrical consumers is defined as follows:

$$h_{Pel} = \frac{P_{el}}{\dot{m}_{H_2}^{product}} \tag{16}$$

The thermodynamic modelling of the heat integration of the NH_3 cracker was performed in Ebsilon.

The remainder of this section is divided into four subsections:

- Model validation of an NH_3 cracker (Subsection 5.1)
- Definition of a reference case based on the current large-scale implementation of an NH_3 cracker (referred to as the 'best guess' case in Subsection 5.2)
- Parameter variations and adaptions of the 'best guess' case for the integration of external ambient heat and heat from the HT-TES-P2H system (Subsection 5.3)
- A simplified economic analysis with and without the proposed HT-TES-P2H concept for an NH_3 reconversion plant with a capacity of 500 t-H_2/day and a supply chain from Brazil/Australia to DE (Subsection 5.4)

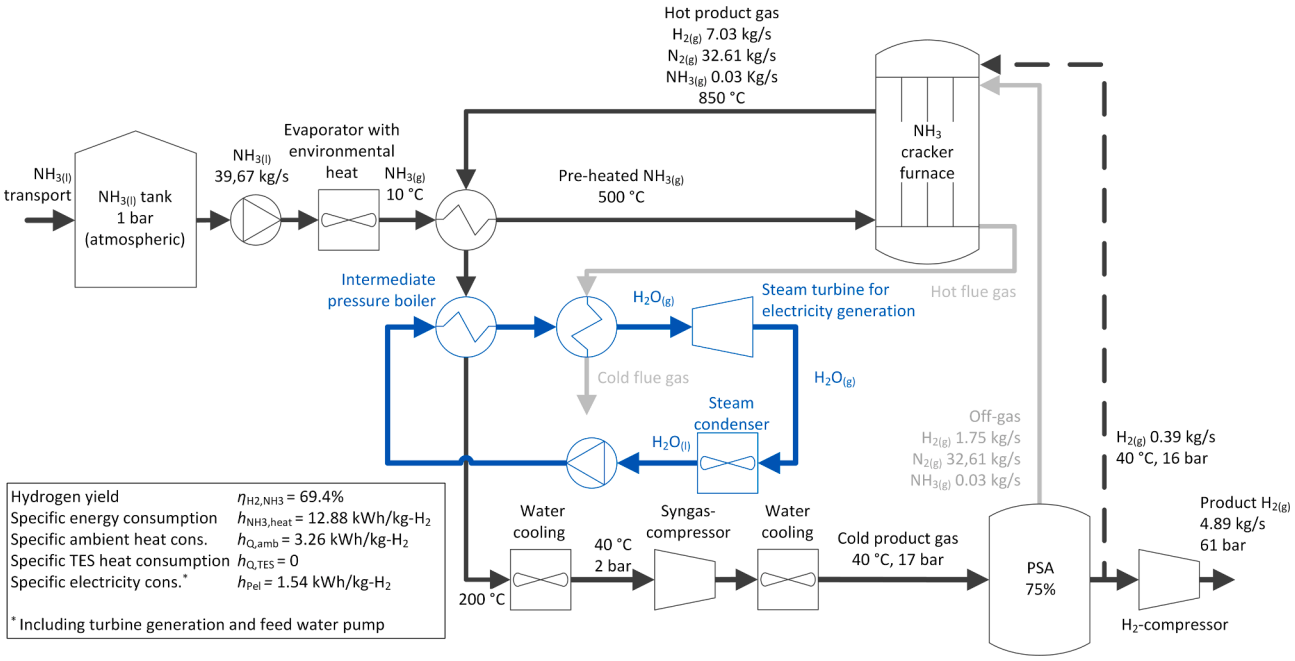

Fig. 8. Process flow diagram illustrating the heat integration of a large-scale reformer type NH_3 cracker from the WE-NET project, used for Ebsilon model validation in this study. PSA, pressure swing adsorption.

5.1. *Modelling validation method*

The design of a large-scale NH_3 cracking unit from a subtask report of the WE-NET project was used for the validation of the Ebsilon model with the following **method** [124,125]. Fig. 8 presents the process flow diagram of the WE-NET project. Ebsilon is a commercial software for industry and research. Ebsilon uses the topology information and specification values of the components to set up a matrix of nonlinear equations, which is first linearised and then solved iteratively using a Gauss-Seidel algorithm [26]. The governing equations for the individual components (e.g., Gibbs reactor) are presented directly in the Ebsilon documentation or previous studies [26]. The property values of the

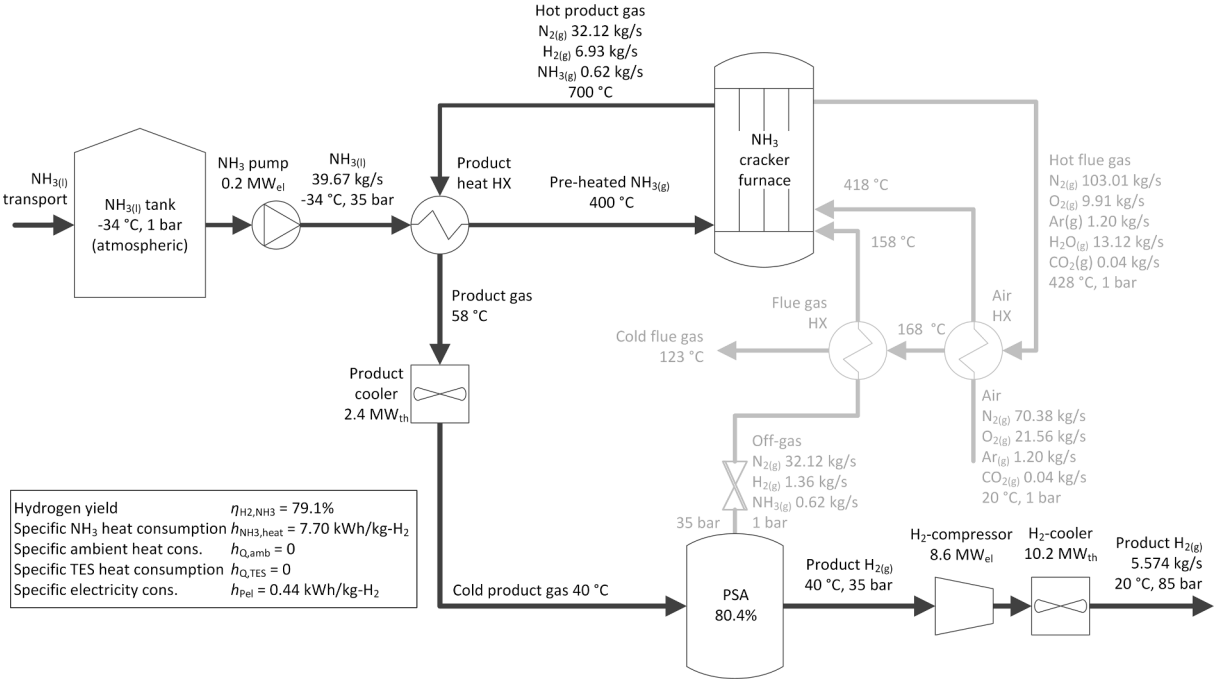

Fig. 9. Process flow diagram illustrating NH_3 cracker heat integration, approximating the current industrial large-scale reformer-type development, referred to as the 'best guess' case. HX, heat exchanger; PSA, pressure swing adsorption.

substances stored in Ebsilon were used. The Ebsilon NH_3 thermochemical equilibrium data for decomposition showed close agreement with the literature values from Appl [67]. Liquid NH_3 was first evaporated under ambient heat at a low NH_3 pressure. The gaseous NH_3 was then preheated to 500 °C with heat from the hot product gas stream. The NH_3 cracker was modelled in Ebsilon using two Gibbs reactors connected in series at 500 and 850 °C with heat integration. Heat was transferred from the hot product gas flow at 850 °C to the cold NH_3 flow and a steam cycle. The residual heat of the hot product gas stream was water-cooled and compressed for the PSA. For all simulations, an idealised isothermal operation of the PSA was assumed. The PSA off-gas and part of the H_2 produced were used to provide combustion heat to the endothermic NH_3 cracker. Finally, the H_2 was compressed to an absolute pressure of 61 bar. Further details on the steam cycle for power generation could not be found in the original publications [124,125].

The **results** of the Ebsilon simulation were compared with the parameters published in the WE-NET project. A direct comparison was not made, as the values between the Ebsilon simulation in this study and the published WE-NET values in the literature were virtually identical. No complete data set was published in the WE-NET project. All reported values [124,125], shown in Fig. 8, were successfully validated. The values for the steam cycle for power generation could not be validated as they were not published in the WE-NET project. In the Ebsilon simulation, approximately 28 MW_{el} was generated by cooling the hot flue gas flow from 511 to 201 °C and cooling the hot product gas from 511 to 200 °C in an intermediate pressure boiler.

5.2. Industrial large-scale 'best guess' reference case

To compare the heat integration approaches analysed in this study, a 'best guess' case was defined as the reference. The 'best guess' case closely aligns with the large-scale industrial development of NH_3 crackers (Table 4). The following **methodological** assumptions and definitions were made for the heat integration process, as shown in Fig. 9:

- As **input** boundary conditions, liquid NH_3 was assumed to be imported (via ship) and stored in an intermediate tank at atmospheric pressure, with a constant NH_3 supply of 36.67 kg-NH_3/s (3168 t-NH_3/day) at −34 °C. This mass flow is consistent with the validation case (Subsection 5.1).
- With an H_2 yield, $\eta_{H2,NH3}$, of 79.1 % (a modelling result), the H_2 product **output** flow was 482 t-H_2/day according to Eq. (9). This value of 482 t-H_2/day can be considered as a typical average for the specified large-scale industrial development portfolio (Table 4). It was assumed that H_2 was fed at ambient temperature into an H_2 network in the future. In DE, a pressure level range of 70–100 bar is considered [132], and an average value of 85 bar was defined. It was assumed that the PSA satisfied the purity requirements.
- For the **H_2 system pressure**, it was assumed that liquid NH_3 was directly pressurised using a pump to a suitable pressure level for a PSA of 35 bar(abs) to omit the compression stages in the gas phase. This assumption matches the typical pressure data for the development of industrial NH_3 crackers (Table 4). As pressure losses do not play a significant role in heat integration, they were neglected for simplification. Furthermore, for simplicity, only large electrical consumers (gas compressors and pumps) were considered.
- Industrial developments typically utilise partial NH_3 conversion with downstream **NH_3 separation**. The usual separation of NH_3 (e.g., H_2O/NH_3 absorption/distillation) upstream of the PSA was not modelled separately due to the small separated NH_3 mass flow, which has a minimal impact on heat integration. The off-gas combustion of the small amount of NH_3 was assumed for simplification.
- In the LT range (400–500 °C), a more expensive Ru-based catalyst can be used. The traditional HT range (700–1000 °C) has disadvantages, as explained in Subsection 4.3.4. There is a general trend in catalyst and cracker development aimed at achieving medium operating **temperatures**. NH_3 cracking was assumed to start at 400 °C as a fixed parameter, which was adopted from Haldor Topsøe. The temperature of 700 °C was selected as the upper fixed limit (Table 4). This presents an average (rather low) value for industrial development and allows for simpler heat integration.
- The **NH_3 cracker furnace** was modelled as a Gibbs reactor. With this approach, it can be expected that the conversion at LTs is overestimated (kinetic limitations are not modelled), and lower NH_3 conversions are achieved overall. To account for this, care was taken when modelling the NH_3 crackers to ensure that there was at least a 20 °C temperature difference at the pinch point. A combustion temperature of up to 1400 °C was assumed, and the combustion air ratio was varied as a free parameter.
- Similar to industrial projects, heat sources (hot product gas and hot flue gas) and sinks (NH_3 evaporator, −preheater, and −cracker) were used for **heat integration**. To avoid overly complex and component-intensive heat integration, and for consistency with industrial development, heat integration was limited to three options:
  1) NH_3 preheating (−34 °C to 400 °C) with the hot product gas
  2) Heating of the NH_3 cracker with PSA off-gas combustion
  3) Off-gas and air preheating by the hot flue gas

  NH_3 evaporation with ambient heat has not yet been adopted by industry and was therefore not included in the 'best guess' case, but was investigated in Subsection 5.3.
- An additional **steam cycle** for the conversion of waste heat into electricity was analysed, but excluded for simplicity due to the low overall increase in energy efficiency for the assumed heat integration.

The **results** of the mass flows, gas compositions, temperatures, and efficiencies are presented in Fig. 9. For the subsequent comparison with other cases, primarily the H_2 yield (Eq. (9)) and the specific NH_3 heat consumption defined in Eq. (13) of the 'best guess' case were used. A typical H_2 yield, $\eta_{H2,NH3}$, value for large-scale industrial NH_3 crackers was 78 % (Table 4), when NH_3 (or produced H_2) was also used to provide heat for the endothermic NH_3 cracker. For the 'best guess' case, a slightly higher but similar value of 79.1 % was achieved. The PSA recovery rate of 80.4 % was similar to the H_2 yield of 79.1 %. The two efficiencies were not entirely identical because small amounts of the NH_3 were not converted in the NH_3 cracker and therefore remained in the off-gas (0.62 kg/s; Fig. 9). The specific NH_3 heat consumption, $h_{NH3,heat}$, was 7.70 kWh/kg-H_2. The total electricity consumption was approximately 8.8 MW_{el}, which results in a specific electricity consumption of $h_{Pel} = 0.44$ kWh/kg-H_2.

5.3. Integration of P2H and TES with parameter variation

The primary objective of the following parameter variation was to thermodynamically model and investigate the technical feasibility of integrating external heat sources (ambient heat and heat from the HT-TES-P2H system) using the 'best guess' case as a reference (Fig. 1, Fig. 9; Subsection 5.2). Compared to the 'best guess' case, additional **methodological** assumptions were made for the following analysis of external heat integration:

- For the NH_3 cracker furnace, the H_2 fraction in the off-gas was at least 5 vol% of the combustion educts to remain within the flammability limit range.
- In the 'progressive' case, no combustion occurred. It was assumed that small quantities of remaining NH_3 in the product gas were recycled and added to the feed stream.
- Compared to the 'best guess' case, the following components were adapted in size or omitted for certain cases: NH_3 pump, NH_3 cracker furnace, product cooler, and PSA, as well as heat exchangers (HXs) for hot product gas, flue gas, and air.

Table 5
Definition of examined modelling cases (columns) along with their assumed input modelling parameters (rows in the upper part of the table) and the modelling results (rows in the lower part of the table). All variables in the table can be compared to those of the 'best guess' case.

Case:	Best guess	Optimised best guess	Ambient heat SoA	TES-P2H heat SoA	Ambient &TES-P2H SoA	Progressive (Ambient + TES-P2H)	Unit
Input/Varied parameter							
NH_3 compressor and evaporator	No	No	Yes	No	Yes	Yes	
NH_3 pre-cracker	No	Yes	Yes	Yes	Yes	Yes	
NH_3-TES cracker	No	No	No	Combi.	Combi.	Yes	
Product cooler	Yes	No	Yes	No	Yes	Yes	
PSA and off-gas combustion	Yes	Yes	Yes	Yes	Yes	No	
Results of NH_3 pre-heating and evaporation							
Ambient heat for NH_3 evaporation	No	No	56.3	No	56.3	56.3	MW_{th}
Hot product gas heat for NH_3 heating	88.7	88.7	22.6	88.7	22.6	23.2	MW_{th}
Results of cracking heat supply							
Flue gas heat for cracking	161.2	158.8	120.5	26.6	26.6	No	MW_{th}
Hot product gas heat for pre-cracking	No	2.4	40.7	2.4	39.3	40.0	MW_{th}
TES heat for cracking	No	No	No	132.2	95.3	123.8	MW_{th}
Share of pre-cracking	0 %	1 %	25 %	1 %	24 %	24 %	
Results of electrical consumption							
NH_3 compressor	No	No	14.3	No	14.3	14.3	MW_{el}
H_2 compressor	8.6	8.7	9.2	10.5	10.5	10.9	MW_{el}
Total electrical consumption	8.8	9.1	23.5	10.7	24.8	25.2	MW_{el}
Results of heat losses							
Product cooler	2.4	No	29.2	No	29.2	29.4	MW_{th}
H_2 cooler	10.2	10.2	10.8	12.3	12.3	12.8	MW_{th}
Flue gas temperature	123	124	132	152	152	No	°C
Results of efficiency, consumption & prod.							
PSA recovery rate	80.4 %	80.7 %	85.4 %	97.5 %	97.5 %	No	
H_2 yield $\eta_{H2,NH3}$	79.1 %	79.4 %	84.1 %	96.0 %	96.0 %	100 %	
Energy eff. with electr. and heat power $\eta_{E,total}$	89.2 %	89.6 %	93.0 %	91.8 %	94.2 %	95.0 %	
Specific NH_3 heat consumption $h_{NH3,heat}$	7.70	7.56	5.54	1.22	1.22	0	kWh/kg-H_2
Specific ambient heat consumption $h_{\dot{Q},amb}$	No	No	2.64	No	2.31	2.22	kWh/kg-H_2
Specific TES heat consumption $h_{\dot{Q},TES}$	No	No	No	5.43	3.92	4.88	kWh/kg-H_2
Specific electricity consumption h_{Pel}	0.44	0.44	1.10	0.44	1.02	1.00	kWh/kg-H_2
Mass flow of H_2 production $\dot{m}_{H_2}^{product}$	5.574	5.595	5.921	6.760	6.760	7.043	kg/s

- Compared to the 'best guess' case, the following additional components were introduced: NH_3 pre-cracker, NH_3 compressor, NH_3-TES combi-cracker, and the HT-TES-P2H system.
- The optimisation of the model cases with respect to these components and their size was adjusted manually. The heat and mass balances were checked using a stationary Ebsilon simulation.
- The key design parameters of the HT-TES-P2H system are the P2H charging power (e.g., MW), the storage capacity (e.g., MWh), and the power (e.g., MW), as well as the outlet and return temperatures, of the discharge unit. A complete modelling of the HT-TES-P2H system was not carried out, as this would have required an annual simulation with a time-series, which is beyond the scope of this study. For the Ebsilon modelling, a constant discharge power and fixed temperatures adapted to the endothermic process were assumed for simplicity. The upper process temperature is the key parameter of the HT-TES-P2H system in this study. The sensitivity was compared for two cases: 565 °C (ambient and TES-P2H SoA case) and 720 °C (progressive case).

Table 5 lists the examined modelling cases (columns) along with their assumed input modelling parameters (rows of the upper part of the table). All variables in the table can be compared to those of the 'best guess' case.

The **results** of the modelled cases are discussed below. The lower part of Table 5 presents the results of the Ebsilon simulations. The discussion focusses on improved H_2 yield, $\eta_{H2,NH3}$, and different specific energy consumptions, as key evaluation criteria for the different heat integration cases. The results are illustrated in Fig. 10, which shows the specific energy consumptions with respect to the H_2 yield. It was assumed that the ambient heat is free or available at a low cost; thus, it was plotted with negative values to distinguish it from other consumptions.

In the **'optimised best guess'** case, the heat integration was improved. For the best 'guess case', thermal losses of 2.4 MW_{th} occurred at the product cooler (Fig. 9). To avoid the cooler, better integration of the hot product gas heat was achieved via an additional NH_3 pre-cracker heated by the hot product gas stream compared to the "best guess" case. The integration of the NH_3 pre-cracker can be observed in a different case, as shown in Fig. 11.

As the avoided product cooler is relatively small compared to the heat consumption, this **results** in only a small improvement in the specific NH_3 heat consumption, from 7.70 to 7.56 kWh/kg-H_2 (2 % improvement).

The **'ambient heat SoA case'** investigated the feasibility of integrating ambient heat for NH_3 evaporation to improve the H_2 yield. NH_3 evaporation was assumed to occur at 5 bar (absolute pressure) and 4 °C, with a seawater supply. This requires an additional evaporator and a relatively power-intensive compressor after evaporation to achieve the same pressure of 35 bar as in the 'best guess' case. For the heat integration shown in the 'best guess' case (Fig. 9), the additional ambient heat introduces excess heat in the hot product gas. This excess heat would be discarded by the product cooler. Therefore, to minimise this effect, an additional NH_3 pre-cracker was introduced. The heat integration for this NH_3 pre-cracker can be observed in a different case, as shown in Fig. 11.

The **results** showed that the specific NH_3 heat consumption significantly improved, decreasing from 7.70 to 5.54 kWh/kg-H_2. This also leads to an increase in the H_2 yield, $\eta_{H2,NH3}$, from 79.1 to 84.1 % (approximately 6 % improvement). However, an additional 14.3 MW_{el} of electricity is required for the NH_3 gas compressor, which heats NH_3 to 177 °C during compression. Due to the integration of ambient heat, part of the hot product gas heat must be cooled (product cooler with a capacity of approximately 29 MW_{th}).

The **'TES-P2H heat SoA'** case considered the integration of HT heat

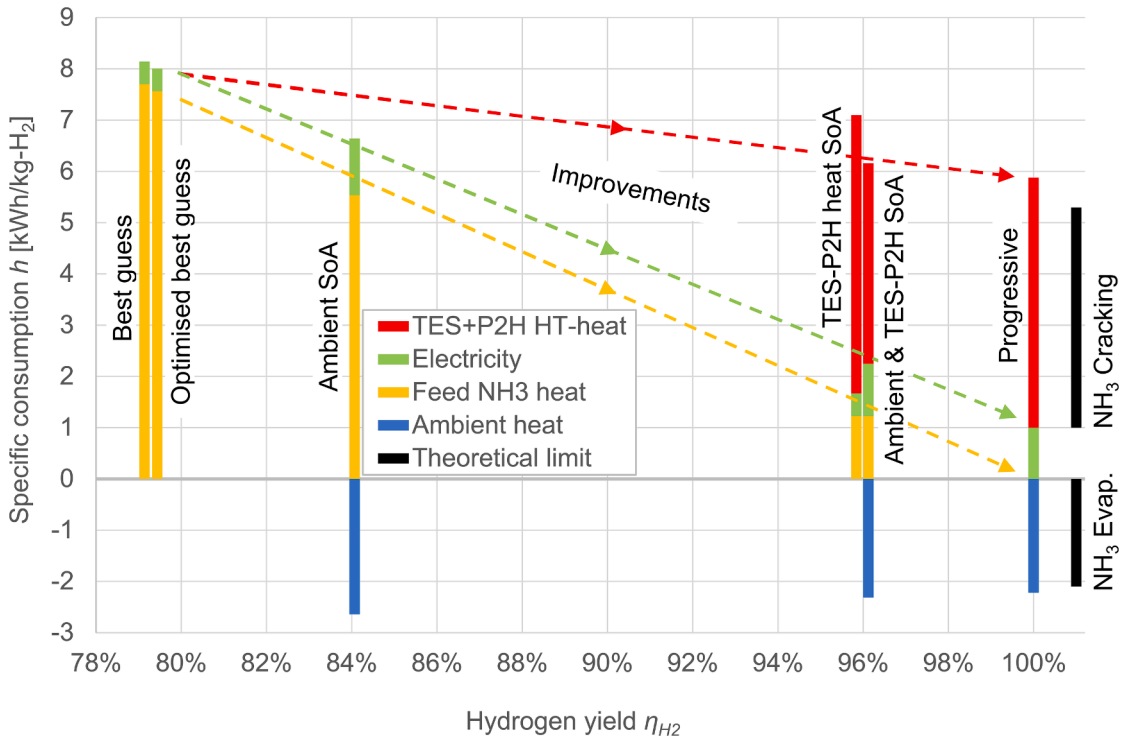

Fig. 10. Comparison of Ebsilon results in terms of specific consumption vs. H_2 yield of all NH_3 cases.

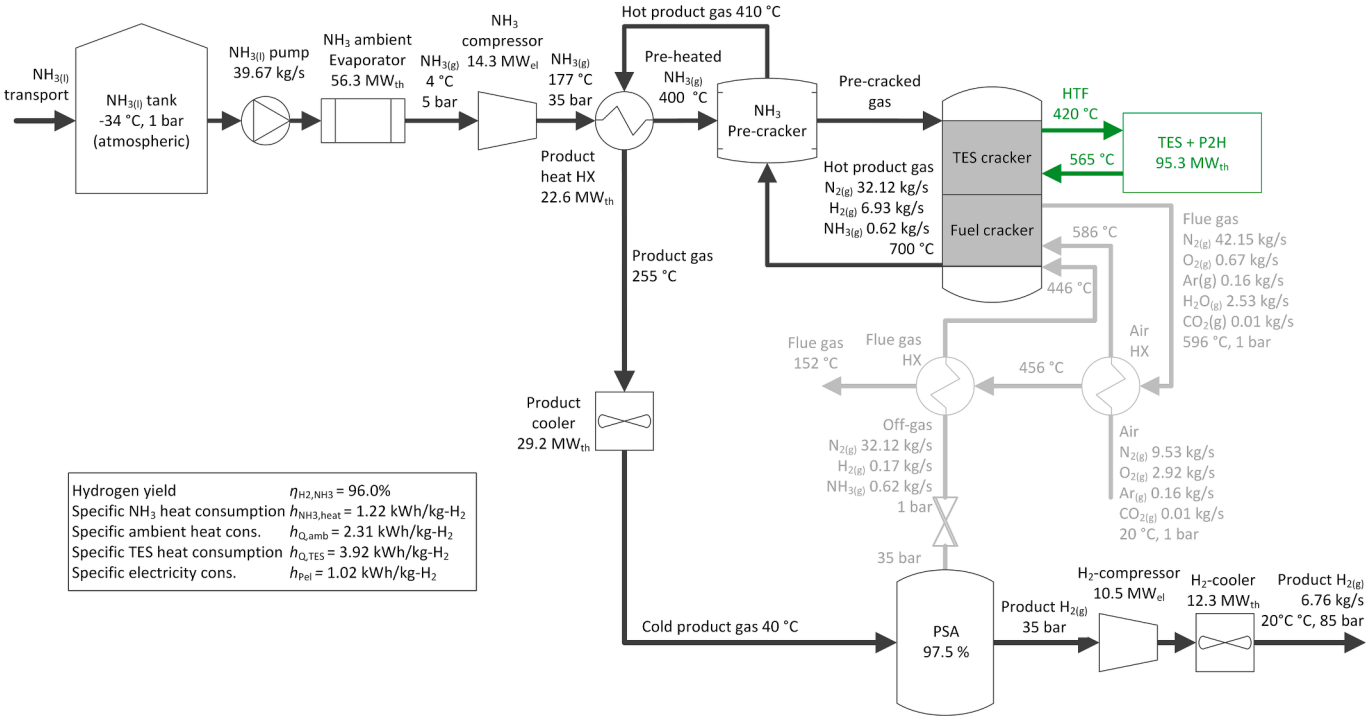

Fig. 11. Process flow diagram illustrating the 'ambient & TES-P2H SoA' case, with external heat supplied from the ambient environment at LT and a TES-P2H system at HT. HX, heat exchanger; P2H, power-to-heat; PSA, pressure swing adsorption; TES thermal energy storage.

from a TES-P2H system into the NH_3 cracking process. The integration of the HT-TES-P2H system can be observed in a different case, as shown in Fig. 11. The minimum and maximum HTF temperatures were assumed to be 420 and 565 °C, respectively. The TES system can be realised using either a molten salt storage tank with molten salt as the heat transfer medium, or a solid media storage system with air as the heat transfer medium (see Subsection 4.1). Due to the temperature limitations of these SoA HT-TES-P2H systems and the required integration of the off-gas, a multi-stage NH_3 cracker system was assumed. The hot part is heated by the combustion system while the colder part is supplied by the TES-P2H system. For the overall thermal optimisation of the system, an additional NH_3 pre-cracker was assumed (as in the 'ambient heat SoA'

case).

The **results** showed that a majority of the energy for the cracking process can be provided by the HT-TES-P2H system. The specific NH_3 heat consumption decreased from 7.70 kWh/kg-H_2 to only 1.22 kWh/kg-H_2. This also led to a significant improvement in H_2 yield, from 79.1 to 96.0 %. The high H_2 yield, $\eta_{H2,NH3}$, was accompanied by a high PSA recovery rate of 97.5 %, which is technically unusual and requires high-level equipment for the separation process. For example, Kumar et al. [81] reported a typical technical PSA range of 65–95 %. A small amount of H_2 in the off-gas can also restrict combustion. The flammability range of H_2 was still fulfilled; however, it did not allow for further gas dilution. The heat in the hot product gas can be fully integrated such that no product cooler is required. Due to the larger quantity of produced H_2, the electricity consumption of the H_2 compressor increases slightly, from 8.6 MW_{el} in the 'best guess' case to 10.5 MW_{el} in the 'TES-P2H heat SoA' case.

In the **'ambient & TES-P2H SoA'** case, the combination of ambient heat and the TES-P2H system was analysed. Fig. 11 depicts the process flow diagram with the following additional components compared to the 'best guess' case: NH_3 evaporator, NH_3 compressor, NH_3 pre-cracker, NH_3-TES combi-cracker, and TES-P2H system.

The **results** showed that the H_2 yield cannot be further increased through a combination of ambient and HT heat, resulting in a high and identical value of 96 %, which is the same as in the 'TES-P2H heat SoA' case. Similar to the 'ambient heat SoA' case, the 'ambient & TES-P2H SoA' case also had the disadvantages of a high power requirement for the NH_3 compressor, along with the same losses at the product cooler of 29 MW_{th}. Both the 'ambient heat SoA' and 'ambient & TES-P2H SoA' cases required the same absolute quantity of ambient heat, approximately 56 MW_{th}. In the 'ambient & TES-P2H SoA' case, however, the amount of produced H_2 was higher, resulting in a decrease in specific ambient heat consumption from 2.64 to 2.31 kWh/kg-H_2. The heat provided by the HT-TES-P2H system dropped significantly from the 'TES-P2H heat SoA' case to the 'ambient & TES-P2H SoA' case. The value decreased from approximately 132 MW_{th} to approximately 95 MW_{th}, or in terms of specific TES heat consumption from 5.43 to 3.92 kWh/kg-H_2. It can therefore be **concluded that the 'ambient & TES-P2H SoA' case is the most favourable**, as it achieved the highest H_2 yield while minimising the amount of external HT heat required, thus reducing the electricity consumption of the TES-P2H system for charging.

The final **'progressive'** case refers to the 'ambient & TES-P2H SoA' case, but deviates from the SoA by assuming technological progress. It was assumed that gas separation could be optimised (e.g., membrane technology) such that no off-gas was produced and combustion could be omitted. It was also assumed that the temperature limitations in the P2H and TES systems can be overcome and that the storage system can provide heat across the overall range of 420–720 °C. This could be achieved, for example, through the development of P2H systems operating above 600 °C and improved salt systems. It is also conceivable that the operating temperature of the NH_3 cracker could be reduced with improved catalysts, though this was not modelled to maintain case comparability.

Compared to the 'ambient & TES-P2H SoA' case, the **results** showed that NH_3 preheating, evaporation, and superheating were nearly identical. The heat from the hot flue gas was replaced by heat from the TES-P2H system, and the H_2 yield could be increased from 96 to 100 % (Table 5). With technical progress, the theoretical potential for 100 % external heat provision for NH_3 evaporation and cracking could be fully exploited. Consequently, the H_2 yield, or the amount of H_2 produced, improved by 20.9 % compared to the 'best guess' case.

Further improvements to the 'progressive' case are possible. In principle, the product cooler can be avoided if NH_3 evaporation is partly performed by the hot product gas heat and partly by ambient heat. This should reduce the ambient heat amount and lower the power consumption of the NH_3 gas compressor. It is also feasible to incorporate LT waste heat (> 85 °C) from surrounding industrial processes in the port area (instead of ambient heat) or LT solar heat for direct NH_3 evaporation at 35 bar and 72 °C. Thus, the electrical energy of the NH_3 gas compressor can be avoided. For both improvements (avoidance of the product cooler and integration of LT waste heat), no significant influence on the relevant H_2 yield was expected. Therefore, modelling was not performed due to the complexity and limited impact on the overall results. It would also be possible to replace all or part of the P2H system, which is fed by PV and wind systems, with a concentrating solar heating system. The investigation of these approaches goes beyond the scope of the work presented here.

5.4. Potential savings of the 'progressive' case

The following discussion provides a simplified estimate of the economic viability of a 500 t-H_2/day NH_3 conversion plant with and without the HT-TES-P2H system. The aim was to determine the capital expenditure (CAPEX) savings for the 'progressive' case compared to the 'best guess' case. For the 'progressive' case, there are significant savings in the exporting country along the process chain, but also smaller additional investments in the importing country for an HT-TES-P2H system, as well as wind and PV systems.

The averaged values were assumed for a green NH_3 supply chain from Brazil/Australia to DE for the year 2030. These two export countries were selected as particularly favourable for DE by Hank. Several major **methodological** assumptions were made based on the studies conducted by Hank et al. [17,44] (also outlined in Table 6):

- Averaged values from three Brazilian and three Australian locations
- Specific PV and wind CAPEX
- Full load hours of wind and PV
- Renewable curtailment share of 16 % (84 % utilisation of renewable power)
- Fixed cost share of 55 % CAPEX for renewables out of the total CAPEX
- Fixed cost share of 14 % for other costs out of the total CAPEX
- Fixed average share of wind generation at 59 % of the total renewable generation
- The conversion efficiencies from renewables to delivered NH_3, based on the annual energy demand and LHV of H_2 and NH_3, are shown in Fig. 12

Separate assumptions were made for the NH_3 reconversion, the HT-TES-P2H system, and the DE renewable electricity supply. The energy efficiencies of NH_3-to-H_2 conversion, based on the LHV, were taken from Table 5 (also shown in Fig. 12). The 'best guess' case served as a reference, with a slightly increased H_2 production capacity from 482 to 500 t-H_2/day (16.7 $GWh_{LHV,H2}$/day) as a round value (Subsection 5.2). A second case, labelled 'progressive + ambient heat', was defined with the same production rate of 500 t-H_2/day for comparison.

It was assumed that the HT-TES discharge unit provides heat for 6000 h/year (68.5 % operation during the year). In the remaining time, the 'ambient heat SoA' case was assumed, which involves operation with both NH_3 combustion and ambient heat provision for the NH_3 cracker. Hence, the 'progressive + ambient heat' case represents a mixed operation of the 'progressive' case, with 6000 h/year using the HT-TES-P2H system, and the remaining 2760 h/year using the 'ambient heat SoA' case without the HT-TES-P2H system (Fig. 12). The following equation defines the mixed energy efficiency of NH_3-to-H_2 conversion based on LHV for the 'progressive + ambient heat' case:

$$\eta_{E,total^*} = \frac{2760\,h}{8760\,h}\eta_{E,total}^{ambient\ heat} + \frac{6000\,h}{8760\,h}\eta_{E,total}^{progressive} \quad (17)$$

where $\eta_{E,total}$ is defined in Eq. (11), which includes electrical power and heat flow from the HT-TES-P2H system. A long, but already realised,

Table 6
Simplified CAPEX analysis for the 'best guess' and 'progressive + ambient heat' cases for DE. The assumptions are referenced, and the remaining values are calculated.

	Best guess	Progressive + ambient heat		Overall savings with installations in Germany (%)
		Export country	Germany	
1) Renewable CAPEX				
Renewable electricity demand	15,249 GWh/year	12,707 GWh/year	612 GWh/year	1931 GWh/year (12.7 %)
Renewable curtailment	16 % [44]	16 % [44]	16 %*	
Renewable electricity with curtailment	18,154 GWh/year	15,127 GWh/year	729 GWh/year	2298 GWh/year (12.7 %)
Wind share of total renewable generation	59 % [44]	59 % [44]	75 %*	
Wind full load hours	3300 h/year [44]	3300 h/year [44]	3300 h/year*	
Wind installed power	3246 MW_{el}	2705 MW_{el}	130 MW_{el}	411 MW_{el} (12.7 %)
Wind specific costs	1300 €/kW [44]	1300 €/kW [44]	1300 €/kW*	
PV full load hours	1800 h/year [44]	1800 h/year [44]	950 h/year*	
PV installed power	4135 MW_{el}	3446 MW_{el}	314 MW_{el}	375 MW_{el} (9.1 %)
PV specific costs	575 €/kW [44]	575 €/kW [44]	575 €/kW*	
2) TES-P2H CAPEX				
P2H unit	Non	Non	204 MW at 150 €/kW*	− 31 Mio€ (spend)
TES-unit	Non	Non	1530 MWh at 50 €/kWh*	−77 Mio€ (spend)
3) Total CAPEX				
Renewable installation	6579 Mio€ (55 % [44])	5497 Mio€ (55 % [44])	350 Mio€	750 Mio€ (11.4 %)
Electrolysis, H_2 storage, air separ., synthesis	3718 Mio€ (31 %)	3098 Mio€	Non	620 Mio€ (16.7 %)
TES-P2H system	Non	Non	107 Mio€	− 107 Mio€ (spend)
Other costs (14 % of total for three columns [44])	1679 Mio€ (14 %)	1399 Mio€	74 Mio€	206 Mio€ (12.2 %)
Total CAPEX	11,995 Mio€ (100 %)	9995 Mio€	532 Mio€	**1468 Mio€ (12.2 %)**

* Assumptions of this study.

TES duration of 15 h was assumed from concentrating solar thermal power plants [61]. For the 500 t-H_2/day 'progressive + ambient heat' case, the heat flow from the HT-TES-P2H system, $\dot{Q}_{TES}$, to the NH_3 cracker was calculated to be 102 MW_{th}. The electrical charging power of the P2H unit was assumed to be twice as high as $\dot{Q}_{TES}$. The exact values for the charging power size and full load hours depend on several factors in future scenarios and can be determined through annual simulations [24,25]. Typical efficiencies of large-scale TES and P2H units are high (~99 %); therefore, losses were neglected, which is a good approximation. The product of $\dot{Q}_{TES}$ and a storage duration of 15 h resulted in a TES capacity of 1530 MWh_{th}. This capacity, with a temperature spread of 145 °C, can be realised with one cold flat-bottom tank at 420 °C and two hot flat-bottom tanks at 565 °C, using molten salt SoA technology as an example [61]. Several further simplifying assumptions were made for the CAPEX comparison of the 'best guess' and 'progressive + ambient

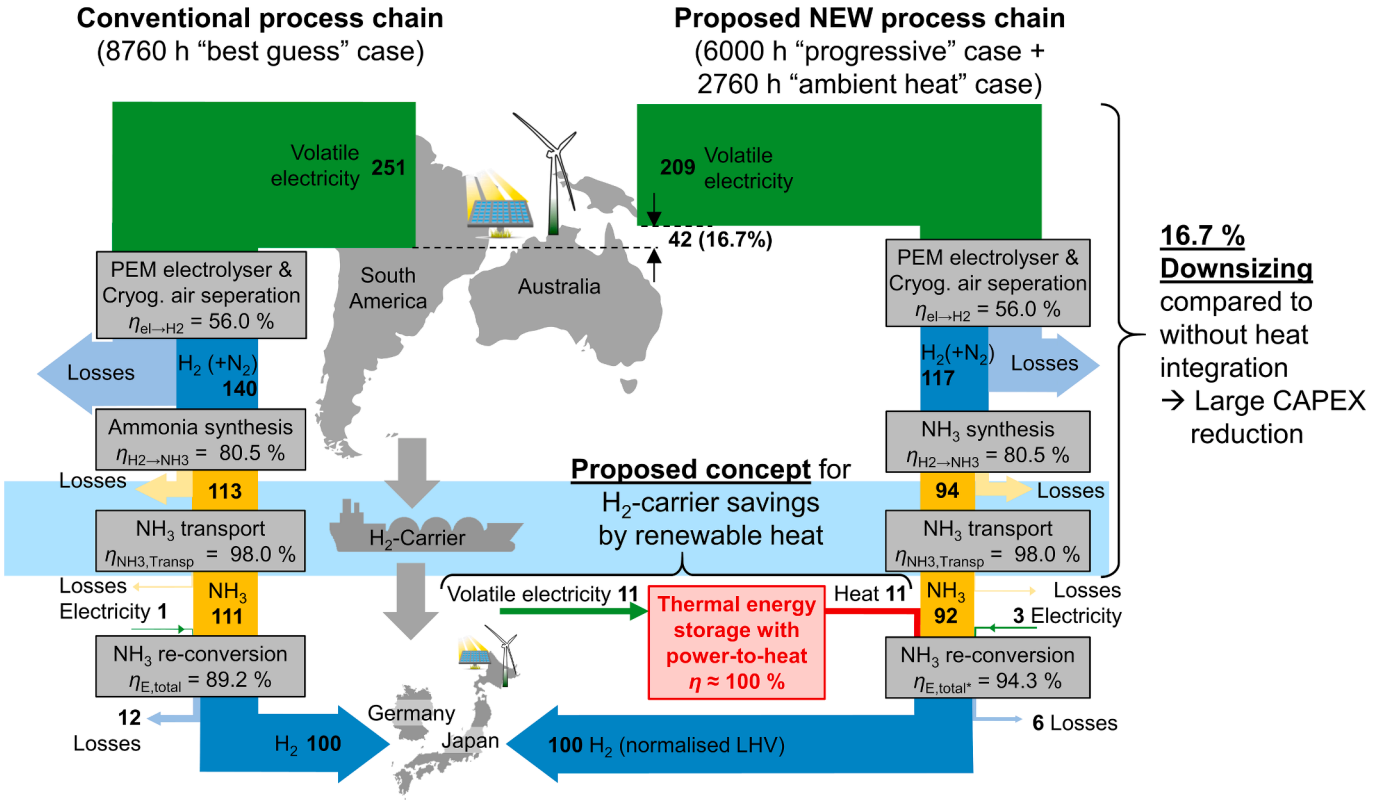

Fig. 12. Sankey diagrams illustrating the 'best guess' case (left) and the 'progressive + ambient heat' case (right), showing the averaged endothermic heat supply from the TES-P2H system (6000 h/year) and conventional NH_3 and ambient heat supply (2760 h/year).

heat' cases (see Table 6 for values):

- 100 % availability for both cases throughout the year. It was assumed that the availability of the NH_3 cracker and the HT-TES-P2H system are the same and that they are operated continuously 24/7 (maintenance intervals were neglected for simplicity).
- Reduced full load PV hours in DE
- Offshore wind with the same full load hours and a higher wind-to-PV share for DE
- Additional savings from reduced port and transport costs were neglected (conservative assumption)
- The same cracker CAPEX was assumed for both cases and thus not included

The annual renewable electricity demand in the exporting country was directly calculated from the H_2 energy LHV for 500 t-H_2/day and the Sankey diagram efficiencies (Fig. 12, Table 5). Table 6 lists the electricity demand values for both cases in the first row. Using electricity demand as a starting point, the values in Table 6 were calculated from top to bottom using the assumptions listed in Table 6. The total CAPEX values for the PV, wind, and HT-TES-P2H systems were calculated. The CAPEX for electrolysis, H_2 storage, air separation, synthesis, and other costs was determined using fixed percentage shares.

Compared to the example for DE, there were minor changes in the **assumptions for JP**. These include the distance to the export country and associated losses, the full load hours of the HT-TES-P2H discharge unit, as well as the full load hours, curtailment, and the ratio of wind and PV in JP. The following deviating assumptions were made for JP compared to DE: JP renewable curtailment of 12 % [133] (instead of 16 % for DE), JP wind share of total renewable generation of 25 % (instead of 59 % for DE), JP full load hour on-shore wind of 2200 h/year (instead of 3300 h/year off-shore for DE), JP full load hour PV of 1000 h/year (instead of 950 h/year for DE).

Overall, the CAPEX study with several simplifying assumptions aims for the examination of basic savings effects. A more detailed analysis and investigation of the sensitivities of the many influencing parameters goes beyond the scope of this study and should be carried out in future studies.

Fig. 12 illustrates the **results** for DE in the form of two Sankey diagrams depicting the annual energy demand using the LHV of H_2 and NH_3. The left-hand diagram shows the 'best guess' case without the HT-TES-P2H system while the right-hand diagram shows the 'progressive + ambient heat' case. The 'progressive + ambient heat' case represents a mixed operation of the 'progressive' case with the HT-TES-P2H system and the 'ambient heat' case without such system. For better readability, the LHV energy quantities were normalised to 100 H_2 units produced. For the 'progressive + ambient heat' case, **a considerable energy and equipment reduction of 16.7 % could be observed along the conversion chain** (Fig. 12). This reduction affects the import country's port infrastructure and shipping capacity, as well as the port infrastructure, NH_3 synthesis plants, water electrolysis, cryogenic air separation, and the installed renewable capacity in the exporting country. These savings of 16.7 % can be verified for plausibility using the H_2 yield, $\eta_{H2,NH3}$. The use of the HT-TES-P2H system reduces the NH_3 quantity by the H_2 yield difference (100 % − 79.1 %) for 6000 h/year (20.9 % · 6000 h/8760 h = 14.3 %). This value of 20.9 % is also approximately consistent with the estimated theoretical potential of 20 % (Subsection 3.3). The difference between 16.7 % and 14.3 % was due to the varying electricity consumption and additional ambient heat utilisation. A further increase in the potential from 16.7 % towards 20 % would be possible with an increase in the annual full load hours (>6000 h) of the HT-TES-P2H system. The exact value of operating hours is part of a techno-economic optimisation, where the CAPEX of the TES plays a significant role. The value of 16.7 % may be increased through the R&D of more cost-effective TES systems (e.g., using natural stone [134]) with longer storage durations, which would allow for higher full load hours.

To compensate for the 16.7 % savings, an additional HT-TES-P2H system and smaller renewable plants are required in the importing country. The next paragraph compares the 16.7 % savings in the supply chain with the additional expenditure for the TES-P2H system and the additional renewable installations in DE (Fig. 12).

Table 6 summarises the simplified CAPEX analysis results for the 'best guess' (second column) and 'progressive + ambient heat' (third and fourth columns) cases. The differences between the two cases are also shown as savings (fifth column; negative values refer to additional expenditures). Table 6 is divided into three parts from top to bottom: 1) renewable generation, 2) the TES-P2H system, and 3) total cost overview. The saving values, given in percentages, refer to the 'best guess' case.

In the following discussion, savings from the 'progressive + ambient heat' case are compared to those from the 'best guess' case. The absolute values in Table 6 result in CAPEX savings of 12.7 % for wind and 9.1 % for PV installations, including the renewable installations in DE. As a rough estimate, for every four wind plants saved in the exporting country, one must be built in DE. In the case of PV systems, two PV systems are saved in the exporting country for every PV system installed in DE. Further significant cost savings of 16.7 % were achieved by downsizing the water electrolysis, cryogenic air separation, H_2 storage, and NH_3 synthesis plants. The capital costs of the additional HT-TES-P2H system were estimated to be 125 million euros, including other additional costs. Overall, despite the additional TES-P2H costs and the extra PV and wind plants in DE, the 16.7 % reduction in the complete conversion chain results in a significant cost saving of 12.2 % or 1468 million euros.

The exemplary analysis for DE in Table 6 was also carried out for JP (not shown in Table 6). This resulted in a similar total cost saving of 11.7 % for JP (compared to 12.2 % for DE). **Significant cost savings of approximately 12 % across the entire value chain from production in the exporting country to H_2 utilisation in** JP **or** DE **were thus calculated.**

6. Conclusions

The aim of this study was to introduce and analyse a new concept to increase the efficiency of importing H_2 carriers. The concept aims to reduce the import volume of the H_2 carrier. Further, the aim of this study was to provide heat for the endothermic reconversion from H_2 carrier to H_2 via a novel HT-TES-P2H system utilising local PV and wind plants. Four H_2 carriers (NH_3, LOHC, MeOH, and LNG) were analysed, with NH_3 considered in detail. The study consisted of three main parts (Sections 3, 4 and 5), where results and conclusions are summarised below.

In this study, **similarities and differences in future H_2 imports were identified for JP and DE** as representative examples of resource-poor industrialised countries (Section 3). This study presents a novel HT-TES-P2H concept for the endothermic reconversion process of imported H_2 derivatives. PV and wind power generated locally in resource-poor importing countries are converted into HT heat using P2H, buffered via a TES system, and fed into an endothermic reconversion process. The key conclusions regarding the import of H_2 derivatives and the proposed HT-TES-P2H concept for reducing H_2 imports are as follows:

- H_2 derivatives – NH_3, LOHC, MeOH, and LNG – are key energy policy options for H_2 import (alongside H_2, either liquefied for ships or compressed for pipelines).
- The proposed HT-TES-P2H concept is applicable to NH_3, LOHC, MeOH, and LNG because all four H_2 carriers have an endothermic reconversion process.
- DE plans to import part of the H_2 via pipelines, whereas JP relies on ship imports; therefore the market potential of the proposed HT-TES-P2H concept could be greater for JP.
- It is proposed to install the HT-TES-P2H system and the endothermic reconversion unit (for H_2 carrier to H_2 conversion) near the port.

Transporting a larger steady flow of H_2 is more economical than transporting volatile wind and PV electricity.
- Suitable regions include the sparsely populated western and north-western regions of JP and the North Sea region of DE.
- In JP, PV plays a greater role than wind in charging the proposed HT-TES-P2H system than it does in DE.

In Section 4, the advantages, disadvantages, and **key features of the four H_2 derivatives** (LOHC, MeOH, LNG, and NH_3) were reviewed and summarised. Additionally, the thermal and process-related integration of TES-P2H systems into the four endothermic conversion processes was analysed systematically and comparatively. This led to the following conclusions:

- The four H_2 carriers – NH_3, LOHC, MeOH, and LNG – have similar theoretical heat demands, in a range of 18–27 % of the produced H_2 LHV. These values include the evaporation energies of the derivatives and water, where applicable. Therefore, the proposed HT-TES-P2H concept could have similar potential for all four H_2 carriers.
- Among other drawbacks, the low market penetration and limited prior experience with LOHC as an H_2 carrier can pose significant hurdles, particularly for its rapid, large-scale market introduction.
- The primary disadvantages of LNG and MeOH reconversion are the effort involved in CO_2 handling and the significant energy required for water evaporation.
- The integration of ambient heat for H_2 derivative evaporation is common for LNG, but has rarely been considered for increasing the efficiency of large-scale industrial NH_3 crackers.
- Suitable technical heat integration concepts for the proposed HT-TES-P2H system were identified for all four H_2 derivatives in this study.
- Four different HT-TES technologies were identified for the proposed HT-TES-P2H concept and the four different H_2 derivatives. The selection of HT-TES technology depends, in particular, on the required lower- and upper-temperature levels, as well as TES market maturity. Thermochemical and latent storage systems are advantageous for processes with narrow temperature windows, whereas sensible TES systems enable rapid large-scale market introduction due to prior experience.
- R&D efforts are necessary to develop endothermic reactors for HTFs, such as molten salts or gases, that are not yet used in this application. Additionally, further R&D is required to advance P2H and molten salt technologies for temperatures exceeding 600 °C to enlarge their application potential (>600 °C is necessary for LNG and NH_3).
- Several scaling steps are required, from R&D work in technical centres, to pilot plants in the application environment, and finally commercialisation. To ensure a timely market launch for the ramp-up of the hydrogen economy, R&D work in the technical centre should begin immediately.
- NH_3 is a key focus of energy policies in JP and DE, has no significant obstacles, and has an existing supply chain. Hence, NH_3 was selected as the most promising H_2 carrier for detailed investigations. Through an in-depth analysis of the large-scale development of NH_3 crackers, a representative 'best guess' cracker heat integration concept was defined.

In Section 5, the **heat and process integration for the reconversion of NH_3 to H_2** using external heat sources was thermodynamically modelled and analysed in detail using the Ebsilon software, leading to the following conclusions:

- A representative large-scale industrial 'best guess' NH_3 cracker with optimised heat integration achieves an H_2 yield of approximately 80 % and consumes 20 % of the NH_3 for heat supply (including endothermic cracking, NH_3 evaporation, and losses).
- The H_2 yield could be increased from 80 to 100 % by integrating external heat.
- Combining ambient heat for NH_3 evaporation with HT heat from the HT-TES-P2H system for the NH_3 cracking process is considered beneficial. The integration of ambient heat allows partial pre-cracking using the hot product gas stream. This enables the HT-TES-P2H system, including the local renewable energy supply, to be reduced in size.
- Based on current SoA, an H_2 yield of 96 % could be achieved using a ceramic regenerator or molten salt TES. An H_2 yield of 100 % also appears feasible with advancements in R&D (e.g., improved gas separation, TES-P2H components for higher operating temperatures, or catalysts for lower operating temperatures).

The **potential** was analysed as an example of NH_3 imports from Brazil/Australia to DE, along with a 500 t H_2/day NH_3 cracker heated via an HT-TES-P2H system. The following conclusions were drawn:

- The maximum **theoretical and technical savings potential** is reduced from approximately **20 %** to an **economical potential of 16.7 %** due to the limited annual full load hours of the HT-TES-P2H system required for economic operation. The significant savings of 16.7 % are related to the energy amount and plant capacity for the entire conversion chain (port infrastructure, shipping, NH_3 synthesis plants, water electrolysis, cryogenic air separation, and installed renewable capacity).
- A simplified CAPEX analysis compared the 16.7 % savings across the entire conversion chain with the additional investments for the HT-TES-P2H system and the added renewables in DE. The savings of 2000 million euros along the conversion chain are considerably greater than the additional investment of 532 million euros for the HT-TES-P2H system and renewables in DE. This resulted in an overall **CAPEX reduction potential of 12.2 %**.
- A similar CAPEX reduction potential of 11.7 % was obtained for JP (compared to 12.2 % in DE). It can therefore be expected that the potential for CAPEX savings for other importing countries for H_2 derivatives is of a similar order of magnitude.
- In addition to potential CAPEX savings, the proposed HT-TES-P2H concept would also increase self-sufficiency in resource-poor industrialised countries (e.g., a 16.7 % reduction in NH_3 imports).
- The 16.7 % reduction in components along the value chain would also have a positive impact on the sustainable development of a future H_2 supply chain. For example, resources for energy-intensive raw materials, such as concrete, steel, and glass, which are required for harbours, ships, and chemical plants, as well as PV and wind plants, could be saved. These and other resource savings could be quantified in future studies.

Overall, the study shows that significant cost savings are possible along the entire value chain when importing H_2 carriers. This can be achieved through local provision of HT heat for the endothermic reconversion process of the H_2 carrier to H_2. The HT heat can be supplied via a novel HT-TES-P2H system that uses local volatile wind and PV electricity. An immediate start to R&D in technical centres and pilot-scale plants for both HT-TES-P2H systems and adapted endothermic reactors are required for timely commercial market launch.

CRediT authorship contribution statement

Thomas Bauer: Writing – review & editing, Writing – original draft, Visualization, Validation, Supervision, Project administration, Methodology, Investigation, Funding acquisition, Formal analysis, Data curation, Conceptualization. **Marco Prenzel:** Writing – review & editing, Validation, Methodology, Investigation, Formal analysis, Data curation, Conceptualization. **Shigehiko Funayama:** Writing – review & editing, Validation, Investigation. **Yukitaka Kato:** Writing – review & editing,

Visualization, Investigation, Funding acquisition.

Declaration of competing interest

The authors declare that they have no known competing financial interests or personal relationships that could have appeared to influence the work reported in this paper.

Acknowledgements

The authors thank the Japan Society for the Promotion of Science (JSPS) for financial support provided for this research under fellowship L24533.

Data availability

Data will be made available on request.

References

[1] Hossain Bhuiyan MM, Siddique Z. Hydrogen as an alternative fuel: a comprehensive review of challenges and opportunities in production, storage, and transportation. Int J Hydrogen Energy 2025;102:1026–44. https://doi.org/10.1016/j.ijhydene.2025.01.033.
[2] Bouckaert S, Pales AF, McGlade C, Remme U, Brent W, Varro L, et al., T. Net Zero by 2050 - A Roadmap for the Global Energy Sector, 4th revision; International Energy Agency (IEA), 2021 https://www.iea.org/ [accessed 17 May 2025].
[3] Esfeh SK, Monnerie N, Mascher S, Baumstark D, Kriechbaumer D, Neumann N, et al. Zukünftige maritime Treibstoffe und deren mögliche Importkonzepte - Kurzstudie (Future maritime fuels and their possible import concepts - short study); German Aerospace Center (DLR), Institute of Maritime [accessed 7 January 2025] Energy Syst 2022. https://elib.dlr.de/186857/2/kurzstudie-maritime-treibstoffe.pdf.
[4] Said SAM, Waseeuddin M, Simakov DSA. A review on solar reforming systems. Renew Sustain Energy Rev 2016;59:149–59. https://doi.org/10.1016/j.rser.2015.12.072.
[5] Hydrogen Insights - A perspective on hydrogen investment, market development and cost competitiveness; Hydrogen Council, 2021. https://hydrogencouncil.com/wp-content/uploads/2021/02/Hydrogen-Insights-2021.pdf [accessed 7 January 2025].
[6] Ammoniak als Energieträger für die Energiewende (Ammonia as an energy source for the energy transition); World Energy Council (WEC), 2023. https://www.weltenergierat.de/wp-content/uploads/2024/01/WEC_Ammoniakstudie_2023.pdf [accessed 7 January 2025].
[7] Import Strategy for hydrogen and hydrogen derivatives; German Federal Ministry for Economic Affairs and Climate Action (BMWK), 2024. https://www.bmwk.de/Redaktion/EN/Hydrogen/Dossiers/national-hydrogen-strategy.html [accessed 7 January 2025].
[8] Jackson C, Fothergill K, Gray P, Haroon F, Makhloufi C, Kezibri N, et al. Ammonia to green hydrogen project; engie, siemens energy [accessed 7 January 2025] Ecuity Consulting, UK's Science & Technology Facilities Council 2020. https://assets.publishing.service.gov.uk/government/uploads/system/uploads/attachment_data/file/880826/HS420_-_Ecuity_-_Ammonia_to_Green_Hydrogen.pdf.
[9] Abdin Z, Tang C, Liu Y, Catchpole K. Large-scale stationary hydrogen storage via liquid organic hydrogen carriers. iScience 2021;24(9):102966. https://doi.org/10.1016/j.isci.2021.102966.
[10] Aziz M. Liquid hydrogen: a review on liquefaction, storage, transportation, and safety. Energies 2021;14(18):5917. https://doi.org/10.3390/en14185917.
[11] Gielen D, Blanco H. Global hydrogen trade to meet the 1.5°C climate goal: part II – technology review of hydrogen carriers [accessed 7 January 2025] Int Renew Energy Agency (IRENA) 2022;ISBN:978-92-9260-431-8. https://www.irena.org/publications/2022/Apr/Global-hydrogen-trade-Part-II.
[12] Merten F, Scholz A, Krüger C, Heck S, Girard Y, Mecke M, et al. Bewertung der Vor- und Nachteile von Wasserstoffimporten im Vergleich zur heimischen Erzeugung – Update (Assessment of the advantages and disadvantages of hydrogen imports compared to domestic production - update); Wuppertal Institut für Klima, Umwelt [accessed 7 January 2025] Energie GmbH 2021. https://wupperinst.org/fileadmin/redaktion/downloads/projects/LEE-H2-Studie.pdf.
[13] Jiao F, Al Ghafri S, O'Neill KT, Stanwix PS, Sellner GM, Fridjonsson EO, et al. Review of hydrogen ortho–para conversion: experimental data and reaction kinetics. React Chem Eng 2024;9(11):2846–62. https://doi.org/10.1039/D4RE00259H.
[14] Heuser P-M, Ryberg DS, Grube T, Robinius M, Stolten D. Techno-economic analysis of a potential energy trading link between Patagonia and Japan based on CO2 free hydrogen. Int J Hydrogen Energy 2019;44(25):12733–47. https://doi.org/10.1016/j.ijhydene.2018.12.156.
[15] Sterner M, Hofrichter A, Meisinger A, Bauer F, Pinkwart K, Maletzko A, et al. 19 import options for green hydrogen and derivatives - an overview of efficiencies and technology readiness levels. Int J Hydrogen Energy 2024;90:1112–27. https://doi.org/10.1016/j.ijhydene.2024.10.045.
[16] Niermann M, Drünert S, Kaltschmitt M, Bonhoff K. Liquid organic hydrogen carriers (LOHCs) – techno-economic analysis of LOHCs in a defined process chain. Energ Environ Sci 2019;12(1):290–307. https://doi.org/10.1039/C8EE02700E.
[17] Hank C, Sternberg A, Köppel N, Holst M, Smolinka T, Schaadt A, et al. Energy efficiency and economic assessment of imported energy carriers based on renewable electricity. Sustainable Energy Fuels 2020;4(5):2256–73. https://doi.org/10.1039/D0SE00067A.
[18] Staudt C, Hofsäß C, von Lewinski B, Mörs F, Prabhakaran P, Bajohr S, et al. Process engineering analysis of transport options for green hydrogen and green hydrogen derivatives. Energ Technol 2024;2301526. https://doi.org/10.1002/ente.202301526.
[19] Shafie P, DeChamplain A, Lepine J. Thermal ammonia decomposition for hydrogen-rich fuel production and the role of waste heat recovery. Int J Energy Res 2024;2024(1):9534752. https://doi.org/10.1155/2024/9534752.
[20] Valera-Medina A, Xiao H, Owen-Jones M, David WIF, Bowen PJ. Ammonia for power. Prog Energy Combust Sci 2018;69:63–102. https://doi.org/10.1016/j.pecs.2018.07.001.
[21] Pashchenko D. Low-grade heat utilization in the methanol-fired gas turbines through a thermochemical fuel transformation. Therm Sci Eng Prog 2022;36. https://doi.org/10.1016/j.tsep.2022.101537.
[22] Pashchenko D. Integrated solar combined cycle system with steam methane reforming: thermodynamic analysis. Int J Hydrogen Energy 2023;48(48):18166–76. https://doi.org/10.1016/j.ijhydene.2023.01.284.
[23] Krieger C, Müller K, Arlt W. Coupling of a liquid organic hydrogen carrier system with industrial heat. Chem Eng Technol 2016;39(8):1570–4. https://doi.org/10.1002/ceat.201600180.
[24] Bauer T, Prenzel M, Klasing F, Franck R, Lützow J, Perrey K, et al. Ideal-typical utility infrastructure at chemical sites – definition. Operat Defossil Chem Ing Tech 2022;94(6):840–51. https://doi.org/10.1002/cite.202100164.
[25] Prenzel M, Klasing F, Franck R, Perrey K, Trautmann J, Reimer A, et al. The potential of thermal energy storage for sustainable energy supply at chemical sites. In Proceedings of the International Renewable Energy Storage Conference (IRES 2022), 2023/05/25, 2023; Atlantis Press: pp 383–400. https://doi.org/10.2991/978-94-6463-156-2_25.
[26] EBSILON®Professional Online Documentation. 2024. https://help.ebsilon.com/EN/Calculation.html and https://help.ebsilon.com/EN/ComponentsGeneralCategories.html [accessed 17 May 2025] (accessed.
[27] World Energy Balances; International Energy Agency (IEA), 2024. https://www.iea.org/data-and-statistics/data-product/world-energy-balances-highlights [accessed 7 January 2025].
[28] Kato Y, Koyama M, Fukushima Y, Nakagaki T. Energy technology roadmaps of japan - future energy systems based on feasible technologies beyond 2030. Springer; 2016.
[29] 6th Strategic Energy Plan; Ministry of Economy, Trade and Industry (METI), Japan, 2021. https://www.enecho.meti.go.jp/category/others/basic_plan/pdf/strategic_energy_plan.pdf [accessed 7 January 2025].
[30] Hirata K, Sasaki Y. Getting lost on the road to decarbonization: Japan's big plans for ammonia [accessed 7 January 2025] Climate Integrate 2022. https://climateintegrate.org/wp-content/uploads/2022/12/Japans-Ammonia-Co-firing_E_ver2_June2022.pdf.
[31] Reynolds S, Doleman C. Japan's largest LNG buyers have a surplus problem; Institute for energy economics and financial [accessed 7 January 2025] Analysis 2024. https://ieefa.org/resources/japans-largest-lng-buyers-have-surplus-problem.
[32] Osaki Y, Hughes L Japan: Putting Hydrogen at the Core of its Decarbonization Strategy; Research Institute for Sustainability (RIFS) Potsdam, 2024. https://doi.org/10.48481/rifs.2024.011.
[33] 7th Strategic Energy Plan (Draft); Ministry of Economy, Trade and Industry (METI), Japan, 2024. https://www.enecho.meti.go.jp/ [accessed 24 December 2024].
[34] Sieler RE, Cames L, Schuster B, Borghardt S, La Trobe B. Hydrogen Factsheet – Japan; adelphi, 2021. https://adelphi.de/system/files/mediathek/bilder/H2%20Factsheet%20Japan.pdf [accessed 7 January 2025].
[35] Bogdanov D, Oyewo AS, Mensah TNO, Nishida Y, Saito T, Aikawa T, et al. Energy transition for Japan: pathways towards a 100% renewable energy system in 2050. IET Renew Power Gener 2023;17(13):3298–324. https://doi.org/10.1049/rpg2.12844.
[36] Global Hydrogen Review 2024; International Energy Agency (IEA), 2024. https://www.iea.org/reports/global-hydrogen-review-2024 [accessed 7 January 2025].
[37] Kuriyama A, Liu X, Naito K, Tsukui A, Tanaka Y. Importance of long-term flexibility in a 100% renewable energy scenario for Japan. Sustain Sci 2024;19(1):165–87. https://doi.org/10.1007/s11625-023-01392-3.
[38] The National Hydrogen Strategy; German Federal Ministry for Economic Affairs and Energy (BMWK), 2020. https://www.bmwk.de/Redaktion/EN/Publikationen/Energie/the-national-hydrogen-strategy.pdf?__blob=publicationFile [accessed 7 January 2025].
[39] Kreidelmeyer S, Trachsel T, Mendelevitch R, Wissner N, Sutter J, Friedrichsen N, et al. Systemischer Vergleich verschiedener Wasserstofftransportrouten; Basel, Berlin, Karlsruhe: ; Prognos AG, Öko-Institut e.V., IREES GmbH, BMWK-Vorhaben Wissenschaftliche Unterstützung Klimapolitik und Maßnahmenprogramm (BMWK project Scientific support for climate policy and programme of measures), Funding code 67KE0088, 2023. https://www.oeko.de/publikation/

systemischer-vergleich-verschiedener-wasserstofftransportrouten/ [accessed 7 January 2025].
[40] Fortschrittsmonitor 2024 Energiewende (Progress monitor 2024 energy transition); Bundesverband der Energie- und Wasserwirtschaft e. V. (BDEW), 2024. https://www.bdew.de/energie/fortschrittsmonitor-energiewende-2024/ [accessed 7 January 2025].
[41] Klimaneutrales Deutschland - Von der Zielsetzung zur Umsetzung (Climate-neutral Germany - from target setting to implementation); Agora Think Tanks, 2024. https://www.agora-energiewende.de/publikationen/klimaneutrales-deutschland-studie [accessed 7 January 2025].
[42] Bard, J.; Becker, S.; von Bonin, M.; Fischer, T.; Ganal, H.; Ganal, I.; Gerhardt, N.; Hoffmann, C.; Krautkremer, B.; Pogacar, S.; et al. Energy transition barometer; Fraunhofer Institute for Energy Economics and Energy System Technology IEE, 2018. https://www.herkulesprojekt.de/content/dam/herkulesprojekt/de/documents/Barometer/2018_B_Barometer_e.pdf [accessed 7 January 2025].
[43] Poganietz W-R, Jochem P, Kopfmüller J, Kullmann F, Naegler T, Ross A, et al. Die Energiewende integrativ denken - ESD Policy Brief Anhang (an integrated approach to the energy transition - ESD Policy Brief Annex) [accessed 7 January 2025] Presentation Helmholtz Energy Programm Energiesystemdesign (ESD) 2024. https://energy.helmholtz.de/forschungshighlights/die-energiewende-integrativ-denken/.
[44] Hank C, Holst M, Thelen C, Kost C, Längle S, Schaadt A, et al. Site-specific, comparative analysis for suitable Power-to-X pathways and products in developing and emerging countries [accessed 7 January 2025] Fraunhofer Institute for Solar Energy Systems ISE 2023. https://www.ise.fraunhofer.de/en/publications/studies/power-to-x-country-analyses.html.
[45] Hampp J, Duren M, Brown T. Import options for chemical energy carriers from renewable sources to Germany. PLoS One 2023;18(2):e0262340. https://doi.org/10.1371/journal.pone.0281380.
[46] Ebner M, Fiedler C, Jetter F, Schmid T. Regionalized potential assessment of variable renewable energy sources in Europe. In 16th International Conference on the European Energy Market (EEM), 18-20 Sept. 2019, 2019; pp 1-5. https://doi.org/10.1109/EEM.2019.8916317.
[47] Sakai S, Kutani S. Comparing the basic strategies of Japan and Germany against the energy crisis while aiming to achieve their climate mitigation goals [accessed 7 January 2025] Jpn Energy Trans Council (GJETC) 2023. https://gjetc.org/wp-content/uploads/2023/05/Topical-Paper-Crisis-Reaction_Final.pdf.
[48] International Energy Agency (IEA) Wind Technology Collaboration Programme (TCP), Webpage; 2022. https://iea-wind.org/about-iea-wind-tcp/members/ [accessed 9 January 2025].
[49] Masson G, de l'Epine M, Kaizuka I. Trends in photovoltaic applications 2024; IEA PVPS T1-43:2024 [accessed 7 January 2025] International Energy Agency (IEA) 2024. https://iea-pvps.org/wp-content/uploads/2024/10/IEA-PVPS-Task-1-Trends-Report-2024.pdf.
[50] Energy Sector Management Assistance Program (ESMAP) - Global Photovoltaic power potential by country - Country factsheets; The World Bank 2020. https://documents1.worldbank.org/curated/en/466331592817725242/pdf/Global-Photovoltaic-Power-Potential-by-Country.pdf [accessed 7 January 2025].
[51] Monitoringbericht 2023 (Monitoring report 2023); Bundesnetzagentur, 2023. https://data.bundesnetzagentur.de/Bundesnetzagentur/SharedDocs/Mediathek/Monitoringberichte/MonitoringberichtEnergie2023.pdf [accessed 7 January 2025].
[52] Slowinski R, Sagdur Y, van Rossum R, Kozub A, Overgaag M, et al. European Hydrogen Backbone - Implementation Roadmap - Cross Border Projects and Cost Update; Guidehouse, Netherlands, 2023. https://ehb.eu/page/publications [accessed 7 January 2025].
[53] Wietfeld A, Krieg D, Hajjar T, Mitra S, Meier R. Competitiveness of green hydrogen import pathways for Germany in 2025; Kearney, Uniper, 2021. https://emvg.energie-und-management.de/filestore/newsimgorg/Illustrationen_Stimmungsbilder/Studien_als_PDF/Competitiveness_of_green_hydrogen_import_pathways_for_Germany_in_2025.orig.pdf [accessed 7 January 2025].
[54] Alvik S, Özgün O. Hydrogen forecast to 2050; DNV AS, Norway, 2022. https://www.dnv.com/focus-areas/hydrogen/forecast-to-2050/ [accessed 7 January 2025].
[55] Executive summary of pre-feasibility study by Fluor for: large scale industrial ammonia cracking plant; Commissioned by Port of Rotterdam Authority (PoR), Air Liquide, Aramco, bp, E.ON/Essent, ExxonMobil, Gasunie, Global Energy Storage (GES), HES International, Koole Terminals, Linde Gas, RWE, Sasol, Shell, Uniper, Vopak and VTTI., 2023. https://www.portofrotterdam.com/sites/default/files/2023-05/large-scale-industrial-ammonia-cracking-plant.pdf [accessed 7 January 2025].
[56] Peters S, Abdel-Mageed AM, Wohlrab S. Thermocatalytic ammonia decomposition – status and current research demands for a carbon-free hydrogen fuel technology. ChemCatChem 2023;15(2):e202201185. https://doi.org/10.1002/cctc.202201185.
[57] Elishav O, Mosevitzky Lis B, Valera-Medina A, Grader G. Chapter 5 - storage and distribution of ammonia. in techno-economic challenges of green ammonia as an energy vector, Valera-Medina, A., Banares-Alcantara, R. Eds.; Academic Press, 2020; pp 85-103. https://doi.org/10.1016/B978-0-12-820560-0.00005-9.
[58] Papadias DD, Peng J-K, Ahluwalia RK. Hydrogen carriers: production, transmission, decomposition, and storage. Int J Hydrogen Energy 2021;46(47):24169–89. https://doi.org/10.1016/j.ijhydene.2021.05.002.
[59] DeSantis D, James BD, Houchins C, Saur G, Lyubovsky M. Cost of long-distance energy transmission by different carriers. iScience 2021;24(12):103495. https://doi.org/10.1016/j.isci.2021.103495.
[60] Bauer T. Chapter 1 - Fundamentals of high-temperature thermal energy storage, transfer, and conversion. In Ultra-High Temperature Thermal Energy Storage, Transfer and Conversion, Datas, A. Ed.; Woodhead Publishing, 2021; pp 1-34. https://doi.org/10.1016/B978-0-12-819955-8.00001-6.
[61] Bauer T, Odenthal C, Bonk A. Molten salt storage for power generation. Chem Ing Tech 2021;93(4):534–46. https://doi.org/10.1002/cite.202000137.
[62] Risthaus K, Linder M, Schmidt M. Experimental investigation of a novel mechanically fluidized bed reactor for thermochemical energy storage with calcium hydroxide/calcium oxide. Appl Energy 2022;315:118976. https://doi.org/10.1016/j.apenergy.2022.118976.
[63] Funayama S, Schmidt M, Mochizuki K, Linder M, Takasu H, Kato Y. Calcium hydroxide and porous silicon-impregnated silicon carbide-based composites for thermochemical energy storage. Appl Therm Eng 2023;220:119675. https://doi.org/10.1016/j.applthermaleng.2022.119675.
[64] Deshmukh, Y. V. Industrial Heating - Principles, Techniques, Materials, Applications, and Design; CRC Press, 2005, ISBN: 978-0367392840. https://doi.org/10.1201/9781420027556.
[65] Tsogt N, Gbadago DQ, Hwang S. Exploring the potential of liquid organic hydrogen carrier (LOHC) system for efficient hydrogen storage and transport: a techno-economic and energy analysis perspective. Energ Conver Manage 2024;299:117856. https://doi.org/10.1016/j.enconman.2023.117856.
[66] Runge P, Sölch C, Albert J, Wasserscheid P, Zöttl G, Grimm V. Economic comparison of different electric fuels for energy scenarios in 2035. Appl Energy 2019;233–234:1078–93. https://doi.org/10.1016/j.apenergy.2018.10.023.
[67] Appl, M. Ammonia. In Ullmann's Encyclopedia of Industrial Chemistry, 2011; https://doi.org/10.1002/14356007.a02_143.pub3.
[68] Ott J, Gronemann V, Pontzen F, Fiedler E, Grossmann G, Kersebohm DB, et al. Methanol. In Ullmann's Encyclopedia of Industrial Chemistry 2012. https://doi.org/10.1002/14356007.a16_465.pub3.
[69] Weichenhain U. Hydrogen transportation - The key to unlocking the clean hydrogen economy; Roland Berger GmbH, 2021. https://www.rolandberger.com [accessed 7 January 2025.
[70] Wijayanta AT, Oda T, Purnomo CW, Kashiwagi T, Aziz M. Liquid hydrogen, methylcyclohexane, and ammonia as potential hydrogen storage: comparison review. Int J Hydrogen Energy 2019;44(29):15026–44. https://doi.org/10.1016/j.ijhydene.2019.04.112.
[71] Marquez C, Deign J, Williams H. Marine methanol - future-proof shipping fuel; Methanol Institute, 2023. https://www.methanol.org/wp-content/uploads/2023/05/Marine_Methanol_Report_Methanol_Institute_May_2023.pdf [accessed 7 January 2025.
[72] Al-Breiki M, Bicer Y. Investigating the technical feasibility of various energy carriers for alternative and sustainable overseas energy transport scenarios. Energ Conver Manage 2020;209:112652. https://doi.org/10.1016/j.enconman.2020.112652.
[73] Spatolisano E, Pellegrini LA, de Angelis AR, Cattaneo S, Roccaro E. Ammonia as a carbon-free energy carrier: NH3 cracking to H2. Ind Eng Chem Res 2023;62(28):10813–27. https://doi.org/10.1021/acs.iecr.3c01419.
[74] Lucentini I, Garcia X, Vendrell X, Llorca J. Review of the decomposition of ammonia to generate hydrogen. Ind Eng Chem Res 2021;60(51):18560–611. https://doi.org/10.1021/acs.iecr.1c00843.
[75] Häussinger P, Lohmüller R, Watson AM. Hydrogen, 2. production. In Ullmann's Encyclopedia of Industrial. Chemistry 2011. https://doi.org/10.1002/14356007.o13_o03.
[76] Boscherini M, Storione A, Minelli M, Miccio F, Doghieri F. New perspectives on catalytic hydrogen production by the reforming, partial oxidation and decomposition of methane and biogas. Energies 2023;16(17):Review. https://doi.org/10.3390/en16176375.
[77] Garcia G, Arriola E, Chen W-H, De Luna MD. A comprehensive review of hydrogen production from methanol thermochemical conversion for sustainability. Energy 2021;217:119384. https://doi.org/10.1016/j.energy.2020.119384.
[78] Ashcroft J, Goddin H. Centralised and localised hydrogen generation by ammonia decomposition. Johnson Matthey Technol Rev 2022;66(4):375–85. https://doi.org/10.1595/205651322X16554704236047.
[79] Sisáková K, Podrojková N, Oriňaková R, Oriňak A. Novel catalysts for dibenzyltoluene as a potential liquid organic hydrogen carrier use—a mini-review. Energy Fuel 2021;35(9):7608–23. https://doi.org/10.1021/acs.energyfuels.1c00692.
[80] Ranjekar AM, Yadav GD. Steam reforming of methanol for hydrogen production: a critical analysis of catalysis, processes, and scope. Ind Eng Chem Res 2021;60(1):89–113. https://doi.org/10.1021/acs.iecr.0c05041.
[81] Kumar R, Singh R, Dutta S. Review and outlook of hydrogen production through catalytic processes. Energy Fuel 2024;38(4):2601–29. https://doi.org/10.1021/acs.energyfuels.3c04026.
[82] Lamb KE, Dolan MD, Kennedy DF. Ammonia for hydrogen storage; a review of catalytic ammonia decomposition and hydrogen separation and purification. Int J Hydrogen Energy 2019;44(7):3580–93. https://doi.org/10.1016/j.ijhydene.2018.12.024.
[83] Andriani D, Bicer Y. A review of hydrogen production from onboard ammonia decomposition: maritime applications of concentrated solar energy and boil-off gas recovery. Fuel 2023;352:128900. https://doi.org/10.1016/j.fuel.2023.128900.
[84] Richard S, Ramirez Santos A, Olivier P, Gallucci F. Techno-economic analysis of ammonia cracking for large scale power generation. Int J Hydrogen Energy 2024;71:571–87. https://doi.org/10.1016/j.ijhydene.2024.05.308.

[85] Ganguli A, Bhatt V. Hydrogen production using advanced reactors by steam methane reforming: a review. Front Therm Eng 2023;3. https://doi.org/10.3389/fther.2023.1143987.
[86] Rüde T, Dürr S, Preuster P, Wolf M, Wasserscheid P. Benzyltoluene/perhydro benzyltoluene – pushing the performance limits of pure hydrocarbon liquid organic hydrogen carrier (LOHC) systems. Sustainable Energy Fuels 2022;6(6):1541–53. https://doi.org/10.1039/D1SE01767E.
[87] Dürr S, Zilm S, Geißelbrecht M, Müller K, Preuster P, Bösmann A, et al. Experimental determination of the hydrogenation/dehydrogenation - equilibrium of the LOHC system H0/H18-dibenzyltoluene. Int J Hydrogen Energy 2021;46(64):32583–94. https://doi.org/10.1016/j.ijhydene.2021.07.119.
[88] Stemmler C, Thesen J, Bartusevičiūtė M, Schlögl R, Lösch H, et al. HySupply - a meta-analysis towards a german-australian supply chain for renewable hydrogen; Acatech, 2021. https://www.acatech.de/wp-content/uploads/2020/11/HySupply_WorkingPaper_Meta-Analysis.pdf [accessed 7 January 2025.
[89] Li L, Vellayani Aravind P, Woudstra T, van den Broek M. Assessing the waste heat recovery potential of liquid organic hydrogen carrier chains. Energ Conver Manage 2023;276:116555. https://doi.org/10.1016/j.enconman.2022.116555.
[90] Innovation Outlook: Renewable Methanol; ISBN: 978-92-9260-320-5; Methanol Institute with International Renewable Energy Agency (IRENA), 2021. https://www.irena.org/publications/2021/Jan/Innovation-Outlook-Renewable-Methanol [accessed 7 January 2025].
[91] Lin X, Meng F, Xu ZJ. Electrochemical cracking for releasing hydrogen from methanol. Artif Photosyn 2024. https://doi.org/10.1021/aps.4c00019.
[92] Alberico E, Nielsen M. Towards a methanol economy based on homogeneous catalysis: methanol to H2 and CO2 to methanol. Chem Commun 2015;51(31):6714–25. https://doi.org/10.1039/C4CC09471A.
[93] Jazani O, Bennett J, Liguori S. Carbon-low, renewable hydrogen production from methanol steam reforming in membrane reactors – a review. Chem Eng Process - Process Intesif 2023;189:109382. https://doi.org/10.1016/j.cep.2023.109382.
[94] Papadias DD, Ahmed S, Kumar R, Joseck F. Hydrogen quality for fuel cell vehicles – a modeling study of the sensitivity of impurity content in hydrogen to the process variables in the SMR–PSA pathway. Int J Hydrogen Energy 2009;34(15):6021–35. https://doi.org/10.1016/j.ijhydene.2009.06.026.
[95] Al Ghafri SZS, Revell C, Di Lorenzo M, Xiao G, Buckley CE, May EF, et al. Techno-economic and environmental assessment of LNG export for hydrogen production. Int J Hydrogen Energy 2023;48(23):8343–69. https://doi.org/10.1016/j.ijhydene.2022.11.160.
[96] Ji M, Wang J. Review and comparison of various hydrogen production methods based on costs and life cycle impact assessment indicators. Int J Hydrogen Energy 2021;46(78):38612–35. https://doi.org/10.1016/j.ijhydene.2021.09.142.
[97] Oni AO, Anaya K, Giwa T, Di Lullo G, Kumar A. Comparative assessment of blue hydrogen from steam methane reforming, autothermal reforming, and natural gas decomposition technologies for natural gas-producing regions. Energ Conver Manage 2022;254:115245. https://doi.org/10.1016/j.enconman.2022.115245.
[98] Meloni E, Iervolino G, Ruocco C, Renda S, Festa G, Martino M, et al. Electrified hydrogen production from methane for PEM fuel cells feeding: a review. Energies 2022;15(10):3588. https://doi.org/10.3390/en15103588.
[99] Wismann ST, Engbæk JS, Vendelbo SB, Bendixen FB, Eriksen WL, Aasberg-Petersen K, et al. Electrified methane reforming: a compact approach to greener industrial hydrogen production. Science 2019;364(6442):756–9. https://doi.org/10.1126/science.aaw8775.
[100] Giaconia A, Iaquaniello G, Morico B, Salladini A, Palo E. Techno-economic assessment of solar steam reforming of methane in a membrane reactor using molten salts as heat transfer fluid. Int J Hydrogen Energy 2021;46(71):35172–88. https://doi.org/10.1016/j.ijhydene.2021.08.096.
[101] Yang Y-J, Liu Z, Zhang R-Z, Zhang J-R, Ma X, Yang W-W. Design optimization of a molten salt heated methane/steam reforming membrane reactor by universal design analysis and techno-economic assessment. Int J Hydrogen Energy 2024;69:1236–45. https://doi.org/10.1016/j.ijhydene.2024.05.045.
[102] Yousefi Rizi HA, Shin D. Green hydrogen production technologies from ammonia cracking. Energies 2022;15(21). https://doi.org/10.3390/en15218246.
[103] Cha J, Park Y, Brigljević B, Lee B, Lim D, Lee T, et al. An efficient process for sustainable and scalable hydrogen production from green ammonia. Renew Sustain Energy Rev 2021;152:111562. https://doi.org/10.1016/j.rser.2021.111562.
[104] Trangwachirachai K, Rouwenhorst K, Lefferts L, Faria Albanese JA. Recent progress on ammonia cracking technologies for scalable hydrogen production. Curr Opin Green Sustainable Chem 2024;49:100945. https://doi.org/10.1016/j.cogsc.2024.100945.
[105] Ristig S, Poschmann M, Folke J, Gómez-Cápiro O, Chen Z, Sanchez-Bastardo N, et al. Ammonia decomposition in the process chain for a renewable hydrogen supply. Chem Ing Tech 2022;94(10):1413–25. https://doi.org/10.1002/cite.202200003.
[106] Morlanés N, Katikaneni SP, Paglieri SN, Harale A, Solami B, Sarathy SM, et al. A technological roadmap to the ammonia energy economy: current state and missing technologies. Chem Eng J 2021;408:127310. https://doi.org/10.1016/j.cej.2020.127310.
[107] Schüth F, Palkovits R, Schlögl R, Su DS. Ammonia as a possible element in an energy infrastructure: catalysts for ammonia decomposition. Energ Environ Sci 2012;5(4):6278–89. https://doi.org/10.1039/C2EE02865D.
[108] Kim J, Huh C, Seo Y. End-to-end value chain analysis of isolated renewable energy using hydrogen and ammonia energy carrier. Energ Conver Manage 2022;254:115247. https://doi.org/10.1016/j.enconman.2022.115247.
[109] Chen C, Wu K, Ren H, Zhou C, Luo Y, Lin L, et al. Ru-based catalysts for ammonia decomposition: a mini-review. Energy Fuel 2021;35(15):11693–706. https://doi.org/10.1021/acs.energyfuels.1c01261.
[110] Humphreys J, Tao S. Advancements in green ammonia production and utilisation technologies. Johnson Matthey Technol Rev 2024;68(2):280–92. https://doi.org/10.1595/205651324X16946999404542.
[111] Ao R, Lu R, Leng G, Zhu Y, Yan F, Yu Q. A review on numerical simulation of hydrogen production from ammonia decomposition. Energies 2023;16(2). https://doi.org/10.3390/en16020921.
[112] Busse T, Reinsdorf A. Evonik catalysts – ammonia cracking solution [accessed 23 November 2024] Evonik Catalysts: Live Webinar 2024;21(11):2024. https://www.evonik.com.
[113] Petzold F. Hydrogen transport - ammonia cracking, presentation. In Global Syngas Technologies Council (GSTC), Tucson, Arizona, 26-28 October 2022, 2022; Clariant Catalysts. https://globalsyngas.org/wp-content/conference-presentations/2022/2022-D2-345-H2-Transport-Ammonia-Cracking.pdf [accessed 7 January 2025].
[114] Nielsen R. Topsoes Ammonia cracking technology – Delivering green Hydrogen, Presentation. In Ammonia Energy Conference 2021, Boston, 2021; Haldor Topsoe A/S. https://www.ammoniaenergy.org/wp-content/uploads/2021/11/Rasmus-Topsoe-NH3-cracking-AEA-2021.pdf [accessed 7 January 2025].
[115] Singh MJ, Jacobsen JH. Unlock the full potential of ammonia through ammonia cracking [accessed 7 January 2025] Online Seminar Topsoe A/S 2023. https://video.topsoe.com/webinar-unlock-the-full-potential.
[116] Stylianou E. KBR Ammonia Cracking, H2ACTSM A roadmap from clean energy source to sustainable hydrogen supply. In 36th Nitrogen + Syngas 2023 International Conference & Exhibition, Barcelona 6-8 March 2023, 2023. https://www.kbr.com/sites/default/files/documents/2023-10/TechnicalJournal2023_2022_KBR_Ammonia_Cracking_H2ACT_Roadmap_Clean_Eenrgy_Source_Sustianable_Hydrogen_Supply_0.pdf [accessed 7 January 2025].
[117] Makhloufi C, Kezibri N. Large-scale decomposition of green ammonia for pure hydrogen production. Int J Hydrogen Energy 2021;46(70):34777–87. https://doi.org/10.1016/j.ijhydene.2021.07.188.
[118] Du Z, Liu C, Zhai J, Guo X, Xiong Y, Su W, et al. A review of hydrogen purification technologies for fuel cell vehicles. Catalysts 2021;11(3). https://doi.org/10.3390/catal11030393.
[119] H2RETAKE - an ammonia cracking solution ready to go, Press Release. Topsoe: 2024. https://www.topsoe.com/our-resources/knowledge/our-products/process-licensing/h2retake-process [accessed 7 January 2025].
[120] Renk C. Ammonia cracking – closing the energy value chain, Press Release [accessed 7 January 2025] Thyssenkrupp Uhde 2024. https://www.thyssenkrupp-uhde.com/en/ammonia-cracking.
[121] Restelli F, Spatolisano E, Pellegrini LA, de Angelis AR, Cattaneo S, Roccaro E. Detailed techno-economic assessment of ammonia as green H2 carrier. Int J Hydrogen Energy 2024;52:532–47. https://doi.org/10.1016/j.ijhydene.2023.06.206.
[122] Cesaro Z, Ives M, Nayak-Luke R, Mason M, Bañares-Alcántara R. Ammonia to power: forecasting the levelized cost of electricity from green ammonia in large-scale power plants. Appl Energy 2021;282:116009. https://doi.org/10.1016/j.apenergy.2020.116009.
[123] Pashchenko D, Mustafin R. Ammonia decomposition in the thermochemical waste-heat recuperation systems: a view from low and high heating value. Energ Conver Manage 2022;251:114959. https://doi.org/10.1016/j.enconman.2021.114959.
[124] International Clean Energy System Using Hydrogen Conversion (WE-NET). Subtask 3. Conceptual design of the total system; NEDO-WE-NET-9631; New Energy and Industrial Technology Development Organization (NEDO), Tokyo, Japan, 1997. https://www.osti.gov/etdeweb/servlets/purl/603999 [accessed 7 January 2025].
[125] Ishimoto Y, Voldsund M, Nekså P, Roussanaly S, Berstad D, Gardarsdottir SO. Large-scale production and transport of hydrogen from Norway to Europe and Japan: Value chain analysis and comparison of liquid hydrogen and ammonia as energy carriers. Int J Hydrogen Energy 2020;45(58):32865–83. https://doi.org/10.1016/j.ijhydene.2020.09.017.
[126] Bagg K. Flexible green ammonia synthesis and Large scale ammonia cracking technology by Uhde®, Presentation. AEA Conference, August 2021, 2021; Thyssenkrupp Green Hydrogen and Chemicals Technology. https://www.ammoniaenergy.org/wp-content/uploads/2021/09/thyssenkruppUhde-FlexibleGreenAmmoniaSynthesisCracking-r00.pdf [accessed 7 January 2025].
[127] Why ammonia is the more efficient hydrogen carrier, Press Release. Thyssenkrupp, 2024. https://www.thyssenkrupp.com/en/stories/sustainability-and-climate-protection/why-ammonia-is-the-more-efficient-hydrogen-carrier [accessed 7 January 2025].
[128] Flexigreen(R) MACH2 - Mega Ammonia Cracking H2 Technology, Flyer. Casale: 2024. https://casale.ch/technologies/hydrogen-syngas/ [accessed 7 January 2025].
[129] Renk C. Ammonia cracking: key technology for the green transformation [accessed 7 January 2025] Press Release thyssenkrupp Uhde 2024. https://www.thyssenkrupp.com/en/stories/sustainability-and-climate-protection/ammonia-cracking-key-technology-for-the-green-transformation.
[130] Ammonia Cracking - Converting renewable and low carbon ammonia to hydrogen, Flyer. Air Liquide: 2024. https://www.airliquide.com/sites/airliquide.com/files/2023-03/air-liquide-brief-ammonia-cracking_641c03322249e.pdf [accessed 7 January 2025].
[131] Renk C. Path and challenges to world scale green ammonia production, Presentation. Indo-German Energy Forum - Green Hydrogen-based Chemicals, 22.

March 2022, 2022; Thyssenkrupp. https://energyforum.in/fileadmin/india/media_elements/Presentations/20220322_H2_Chemicals/3_Thyssenkrupp.pdf [accessed 7 January 2025].
[132] Genehmigung eines Wasserstoff-Kernnetzes (Authorisation of a hydrogen core network); Bundesnetzagentur, Germany, 2024. https://www.bundesnetzagentur.de/SharedDocs/Downloads/DE/Sachgebiete/Energie/Unternehmen_Institutionen/Wasserstoff/Genehmigung.pdf [accessed 7 January 2025].
[133] Master plan for cross-regional networks; Organization for Cross-regional Coordination of Transmission Operators, OCCTO, Japan, 2023. https://www.occto.or.jp/kouikikeitou/chokihoushin/files/chokihoushin_23_01_01.pdf [accessed 29 May 2025].
[134] Odenthal C, Klasing F, Knödler P, Zunft S, Bauer T. Experimental and numerical investigation of a 4 MWh high temperature molten salt thermocline storage system with filler. In SolarPaces, Daegu, South Korea 2019. https://doi.org/10.1063/5.0028494.